

LA-10971-MS

UC-4 and UC-25
Issued: November 1987

LA--10971-MS

DE88 005083

Metal Hydrides

Jay R. Carnes
Narzir P. Kherani*

DISCLAIMER

This report was prepared as an account of work sponsored by an agency of the United States Government. Neither the United States Government nor any agency thereof, nor any of their employees, makes any warranty, express or implied, or assumes any legal liability or responsibility for the accuracy, completeness, or usefulness of any information, apparatus, product, or process disclosed, or represents that its use would not infringe privately owned rights. Reference herein to any specific commercial product, process, or service by trade name, trademark, manufacturer, or otherwise does not necessarily constitute or imply its endorsement, recommendation, or favoring by the United States Government or any agency thereof. The views and opinions of authors expressed herein do not necessarily state or reflect those of the United States Government or any agency thereof.

*Guest Scientist at Los Alamos. Ontario Hydro-power, Ontario, CANADA.

MASTER

Los Alamos Los Alamos National Laboratory
Los Alamos, New Mexico 87545

DISTRIBUTION OF THIS DOCUMENT IS UNLIMITED *EB*

DISCLAIMER

This report was prepared as an account of work sponsored by an agency of the United States Government. Neither the United States Government nor any agency thereof, nor any of their employees, makes any warranty, express or implied, or assumes any legal liability or responsibility for the accuracy, completeness, or usefulness of any information, apparatus, product, or process disclosed, or represents that its use would not infringe privately owned rights. Reference herein to any specific commercial product, process, or service by trade name, trademark, manufacturer, or otherwise does not necessarily constitute or imply its endorsement, recommendation, or favoring by the United States Government or any agency thereof. The views and opinions of authors expressed herein do not necessarily state or reflect those of the United States Government or any agency thereof.

DISCLAIMER

Portions of this document may be illegible in electronic image products. Images are produced from the best available original document.

METAL HYDRIDES

by

Jay R. Carnes and Narzir P. Kherani

ABSTRACT

Metal hydride information is not available for most hydrides in a consolidated quick-reference source. This report's objective is to fill the need for such a document providing basic thermodynamic data for as many metal hydrides as possible. We conducted a computerized library search to access as many sources as possible and screened each source for such thermodynamic data as pressure-temperature graphs, van't Hoff curves, and impurity effects. We included any other relevant information and commented on it.

A primary concern to be investigated in the future is the behavior of metal tritides. This would be important in the area of emergency tritium clean-up systems. The hydride graphs are useful, however, as tritides may be expected in most cases to behave similarly and at least follow trends of their respective hydrides.

I. INTRODUCTION

The increased interest in metal hydrides in the last 30 years has prompted research into fabrication of hydrides with desired structural, kinetic, and thermodynamic properties for various applications. Metal hydrides show potential as portable hydrogen sources for combustion engines and as ultrapure hydrogen sources for industry and research. Perhaps the most interesting application of metal hydrides, if not the most researched, lies in the

area of nuclear power. They have been used as moderators, reflectors, and shields in high-temperature mobile nuclear fission reactors.¹ In addition, the tritium containment needs for nuclear fission reactors will be met by metal hydrides.

The term hydride has many definitions, the most basic being a binary compound or mixture of the form A_xH_y produced by metallic interaction with hydrogen. For metal hydrides, A represents a metal or metal alloy, H represents hydrogen or hydrogen isotopes, and x and y represent the stoichiometric combination of A and H. The term compound covers the cases where ionic or covalent bonds are formed between the metal and the hydrogen, whereas the term mixture includes physisorption of hydrogen onto a metal.

Often the metallic hydride formed has properties different from those of the base metal or alloy. Specifically, the hydrides take on different electromagnetic, mechanical, and thermodynamic properties that make them amendable for various applications. Desired metal hydride properties for many applications are

1. H_2 desorption at moderate temperatures (300°C-600°C) with low equilibrium pressures (under 760 mm Hg);
2. high H/M atomic ratio (greater than 1.0);
3. minimal powdering caused by hydrogen sorption;
4. minimal poisoning from oxygen, nitrogen, and hydrocarbons over numerous absorption-desorption cycles;
5. pure gaseous hydrogen liberated at elevated temperatures;
6. easy activation accomplished under vacuum and moderate temperatures;
7. fast absorption kinetics;
8. abundant and inexpensive base metals; and
9. low-density base metal to increase portability.

This report presents a brief survey of most of the currently known metal hydrides. We group the metal hydrides either as pure metals or as alloys. The pure metals are subdivided according to periodic table position, whereas the alloys are subdivided according to the periodic table position of the base element. The hydrides are examined by their pressure-composition-temperature (PCT) diagrams and their van't Hoff curves. The main source of data for the pure metals is Libowitz et. al.,¹ whereas the data for the alloys are obtained from proceedings and journals.

II. PURE METALS

This section discusses equilibrium characteristics of five specific groups of metal hydrides: (1) saline hydrides, (2) Group III A and IV A hydrides, (3) rare-earth hydrides, (4) actinide hydrides, and (5) covalent hydrides and hydrides of Group V through Group VIII transition metals. The periodic table in Fig. 1 illustrates the divisions used in our discussion of metal hydrides in the report.

A. Saline Hydrides

The saline hydrides are so called because of their saltlike bonding in which the hydrogen is present as a negatively charged hydride ion. Thus, in combination with the strongly positive elements of Groups I and II, hydrogen forms strong ionic bonds. Pure beryllium hydride apparently has not been prepared and is excluded from this group.

The hydrides of the alkali metals and alkali earth metals have several common physical and chemical characteristics. All are white or colorless crystalline solids, physically resembling the corresponding halides. All react with water and decompose at moderately high temperatures; each of these reactions liberates hydrogen. They all have melting temperatures considerably above those of the pure metals. When the hydrogen reacts with any of the metals except magnesium, the lattice spacings between the metal atoms contract, creating a higher-density material. Because these hydrides have negative hydrogen atoms, they are reducing agents, which are useful for synthesis of other hydrides. The hydrides of the two heaviest elements of this classification, francium and radium, have not been prepared.

A given amount of hydrogen at a fixed temperature introduced into a metal system provides data for a pressure-composition isotherm. The metal sorbs some of the hydrogen until an equilibrium is reached, at which point the hydrogen pressure is constant. When more hydrogen is added to the system, a new equilibrium pressure is attained as the hydride composition changes. With enough data points, a PCT graph can characterize the metal-hydrogen system at various temperatures.

PCT diagrams shown in Figs. 2-5 represent the Li-H,² Na-H,³ Ca-H,⁴ Mg-H, and Mg-D⁵ systems, respectively. Notes on the figures give the fixed temperatures. The shape of the curves is fairly constant, with plateau pressures well below atmospheric. The saline hydrides exhibit broad plateaus, usually starting at less than 20% hydrogen and extending to near the maximum hydriding capability of the metal. The plateau pressures are essentially constant in this regime.

Saline		Metallic										Covalent	
IA	IIA											IIIB	IVB
LiH	(BeH ₂) ₂ Covalent											Series of Boron Hydrides	
NaH	MgH ₂											(AlH ₃) ₂	Series of Si Hydrides
		IIIA	IVA	VA	VIA	VIIA	VIII A			IB	II B		
KH	CaH ₂	ScH ₂	TiH ₂ (cubic and tetrag.)	VH VH ₂	CrH CrH ₂	Mn —	Fe —	Co —	NiH	CuH	(ZnH ₂) ₂	(GaH ₃) ₂	Series of Ge Hydrides
RbH	SrH ₂	YH ₂ YH ₃	ZrH ₂ (cubic and tetrag.)	NbH NbH ₂	Mo —	Tc —	Ru —	Rh —	PdH	Ag —	(CdH ₂) ₂	(SnH ₃) ₂ (SnH ₂) ₂	SnH ₄ Sn ₂ H ₆
CsH	BaH ₂	See Rare-Earth Series	HfH ₂ (cubic and tetrag.)	TaH	W —	Re —	Os —	Ir —	Pt —	Au —	(HgH ₂) ₂	(PbH ₃) ₂ (PbH ₂) ₂	PbH ₄

Rare-Earth Series

LaH ₂₋₃	CeH ₂₋₃	PrH ₂₋₃	NdH ₂₋₃	Pm ?	SmH ₂ SmH ₃	EuH ₂	GdH ₂ GdH ₃	TbH ₂ TbH ₃	DyH ₂ DyH ₃	HoH ₂ HoH ₃	ErH ₂ ErH ₃	TmH ₂ TmH ₃	YbH ₂ YbH ₃ (?)	LuH ₂ LuH ₃
--------------------	--------------------	--------------------	--------------------	------	--------------------------------------	------------------	--------------------------------------	--------------------------------------	--------------------------------------	--------------------------------------	--------------------------------------	--------------------------------------	--	--------------------------------------

Actinide Series

AcH ₂	ThH ₂ Th ₄ H ₁₃	PaH ₃	UH ₃	NpH ₂ NpH ₃	PuH ₂ PuH ₃	AmH ₂ AmH ₃ (?)
------------------	---	------------------	-----------------	--------------------------------------	--------------------------------------	--

Fig. 1. Periodic table of the elements incorporating metal hydrides.

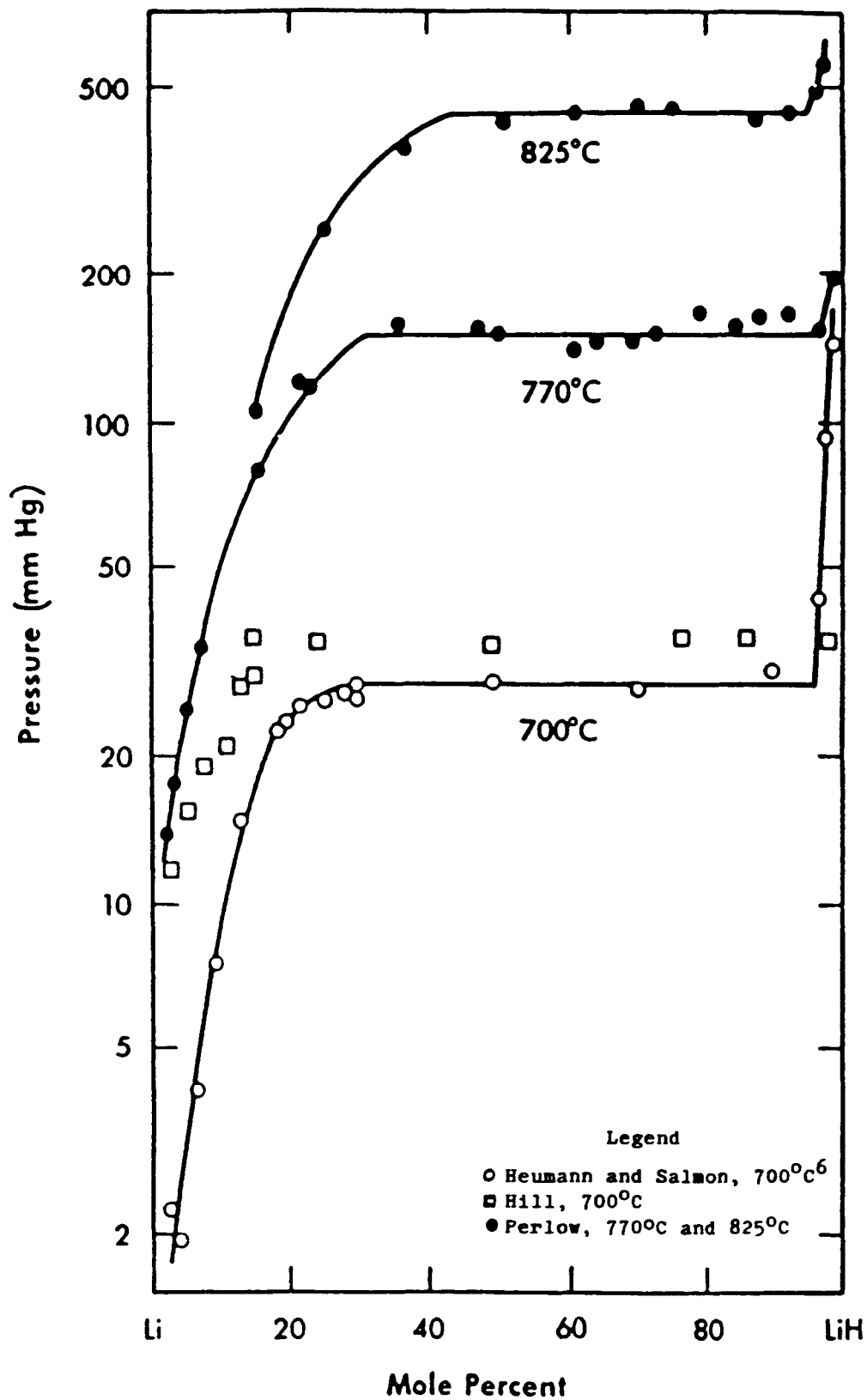


Fig. 2. Pressure-composition isotherms for the lithium-hydrogen system.

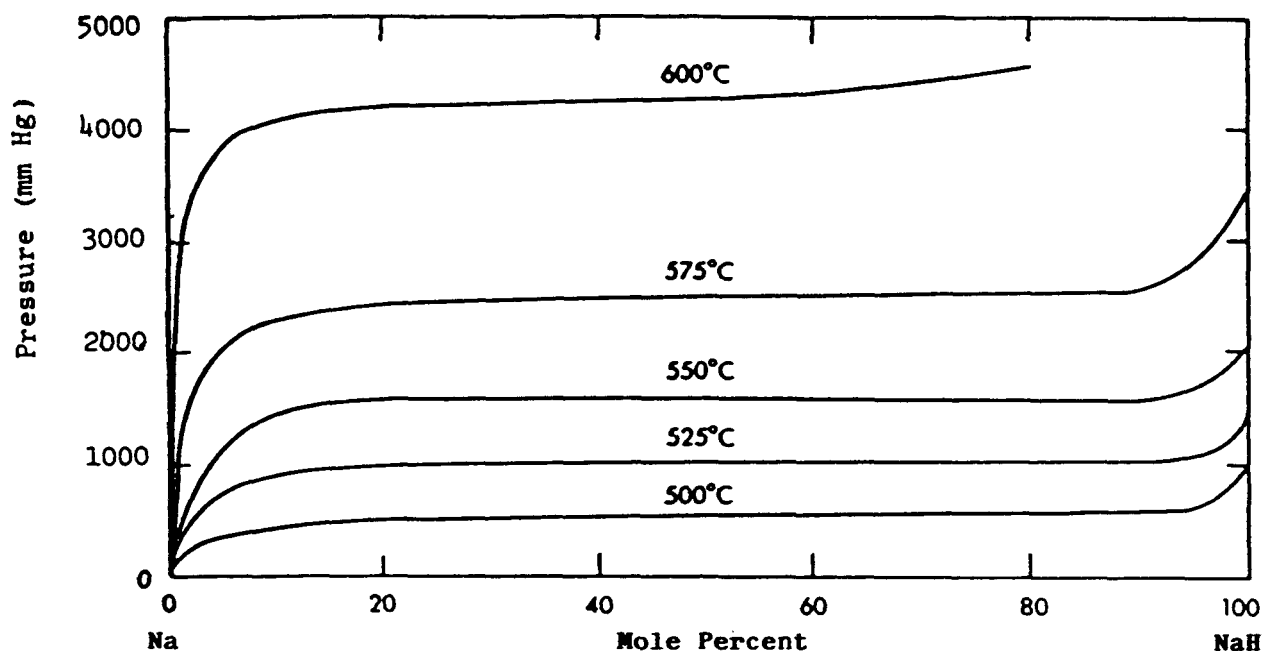


Fig. 3. Pressure-composition isotherms for the sodium-hydrogen system.

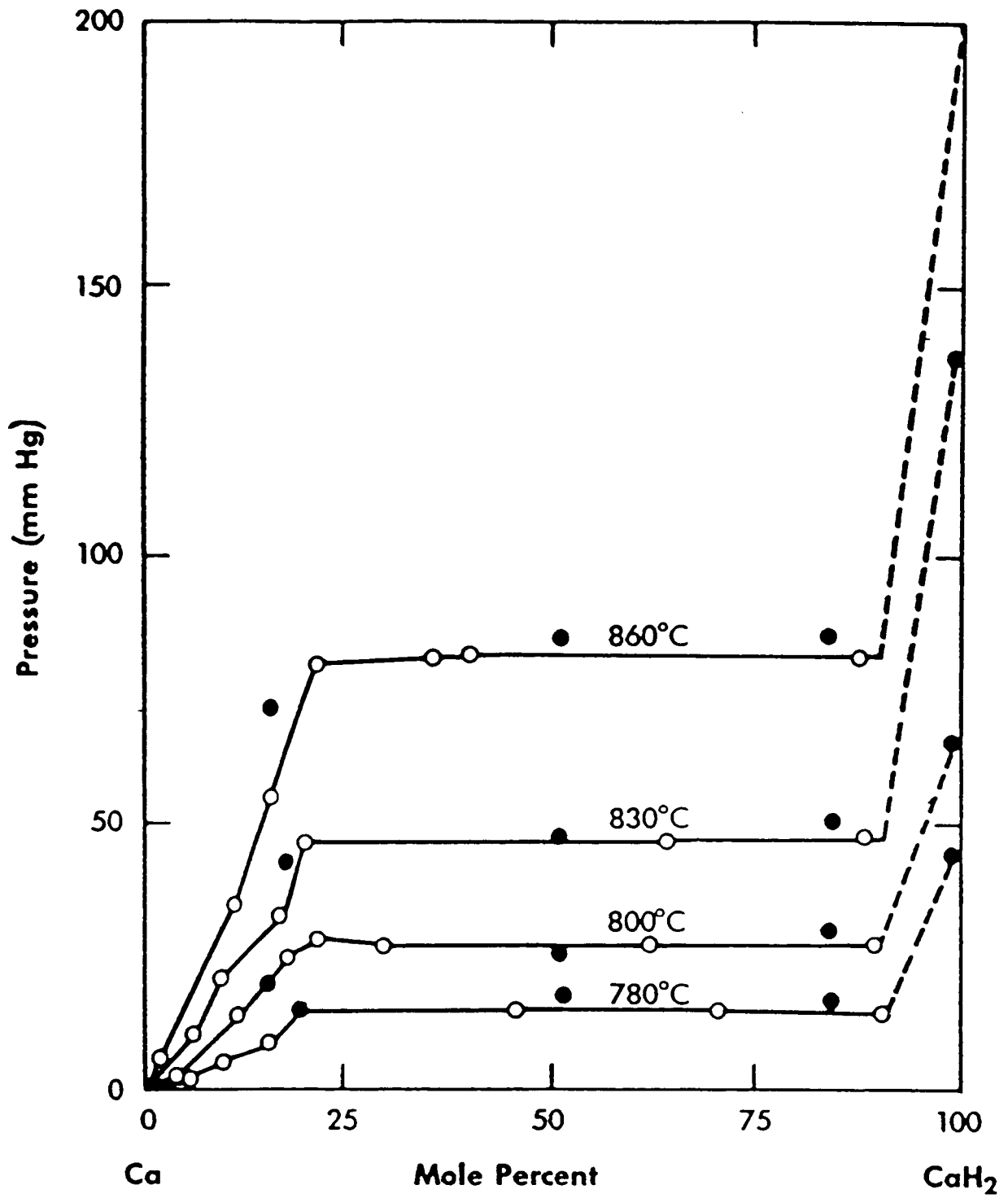


Fig. 4. Pressure-composition isotherms for the calcium-hydrogen system.

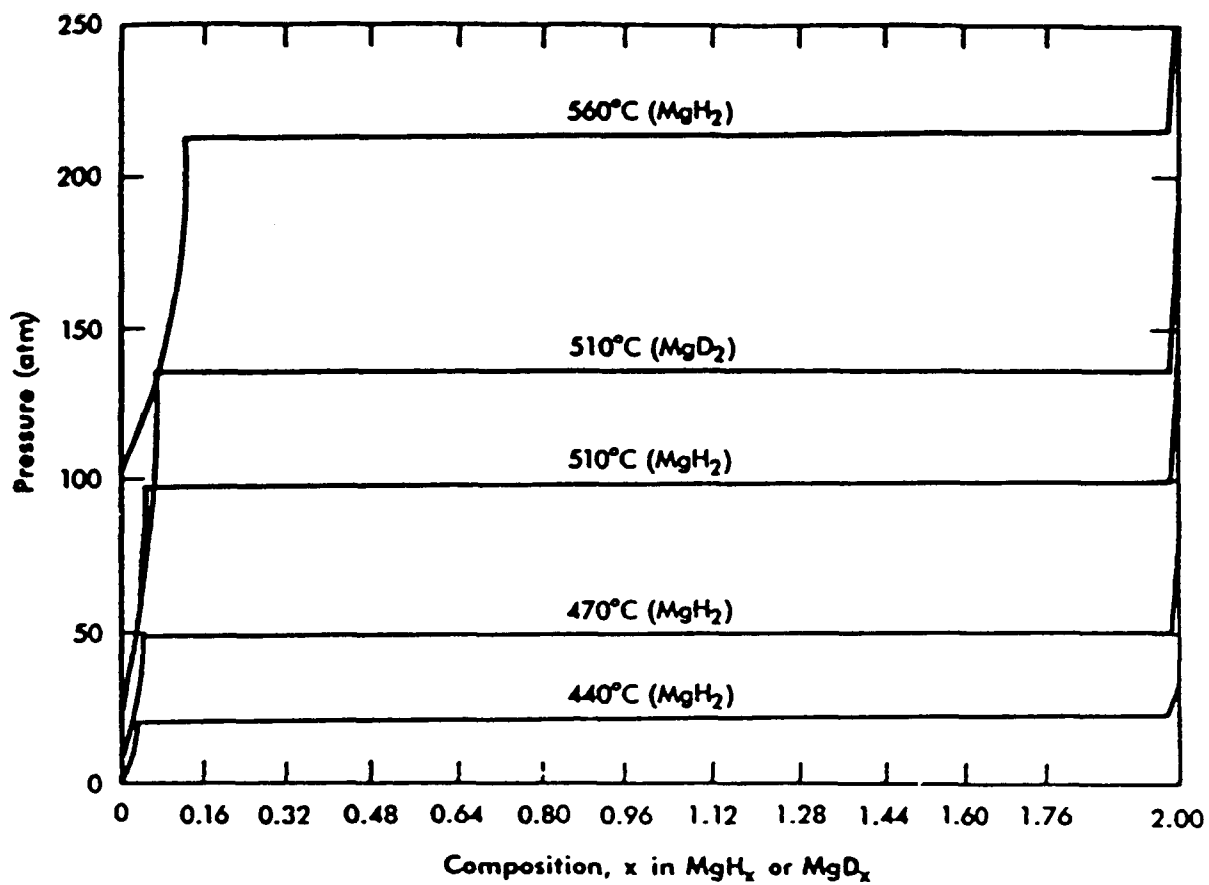


Fig. 5. Pressure-composition isotherms for the magnesium-hydrogen and magnesium-deuterium systems.

For such plateaus, it is convenient to obtain pressure as a function of temperature. Such functions are of the form

$$\log P = -A/T + B \quad (1)$$

where P = pressure (mm Hg),

A = slope,

T = temperature (K), and

B = intercept.

These curves are known as the van't Hoff curves. Table I gives the constant values for the saline hydrides, and Fig. 6 shows these van't Hoff curves.

The van't Hoff curve for the Li-H system comprises data from five investigators. Messer² consolidated the separate results to discover the uniformity of the findings. We believe the best line through the data is that of Heumann and Salmon.⁶

The log P vs $1/T$ curves usually have identical slopes for a given temperature at any hydride composition along a pressure plateau. This is not the case, however, at the extreme right or left of Figs. 2-5, where pressure varies with solid composition. This point is illustrated with the Ca-H system in Fig. 7, from Treadwell and Sticher.⁴ The 50% and 83% lines agree closely, whereas the others do not. The two lines that agree still have slope values that differ by approximately 10%; such differences in the constants A and B are usually found whenever two different people investigate the same hydride. The constants for Ca-H given in Table I are from the research of Curtis and Chiotti.⁷ They determined that a solid-state transformation in the Ca-H phase is responsible for a change in slope of the log P vs $1/T$ curve.

The Na-H line is from the findings of Banus et al.³ and Herold.⁸ Banus investigated the Na-H system from 500°C-600°C, whereas Herold worked from 250°C-415°C.

Stampfer et al.⁵ investigated the Mg-H system over the range 440°C-560°C.

For the rest of the saline hydrides (KH, RbH, CsH, SrH₂, and BaH₂), reliable PCT data are not available over the entire composition range. The curves probably resemble those of the known saline hydrides. Several investigators have determined equilibrium plateau pressures from which they have constructed van't Hoff curves. Banus et al.³ consider Herold's work on the K-H, Rb-H, and Cs-H systems to be the most accurate. Banus et al. also report on the van't Hoff equation for 92.3 mol% Sr-H. Schumb et al.⁹ report on the van't Hoff curve for the Ba-H system.

TABLE I
SALINE HYDRIDE VAN'T HOFF CONSTANTS

<u>System</u>	<u>A</u>	<u>B</u>	<u>Temperature Range (°C)</u>
Li-H	8224.0	9.9258	600-900
Ca-H	9610.0	10.227	600-780
	8890.0	9.481	780-900
Na-H	6100.0	11.66	250-415
	5958.0	11.47	500-600
Mg-H	8950.7	22.88	440-560
K-H	6175.0	11.69	288-415
Rb-H	5680.0	11.80	246-350
Cs-H	5900.0	11.79	245-378
Sr-H	10400.0	11.10	565-900
Ba-H	9150.0	10.4	470-550

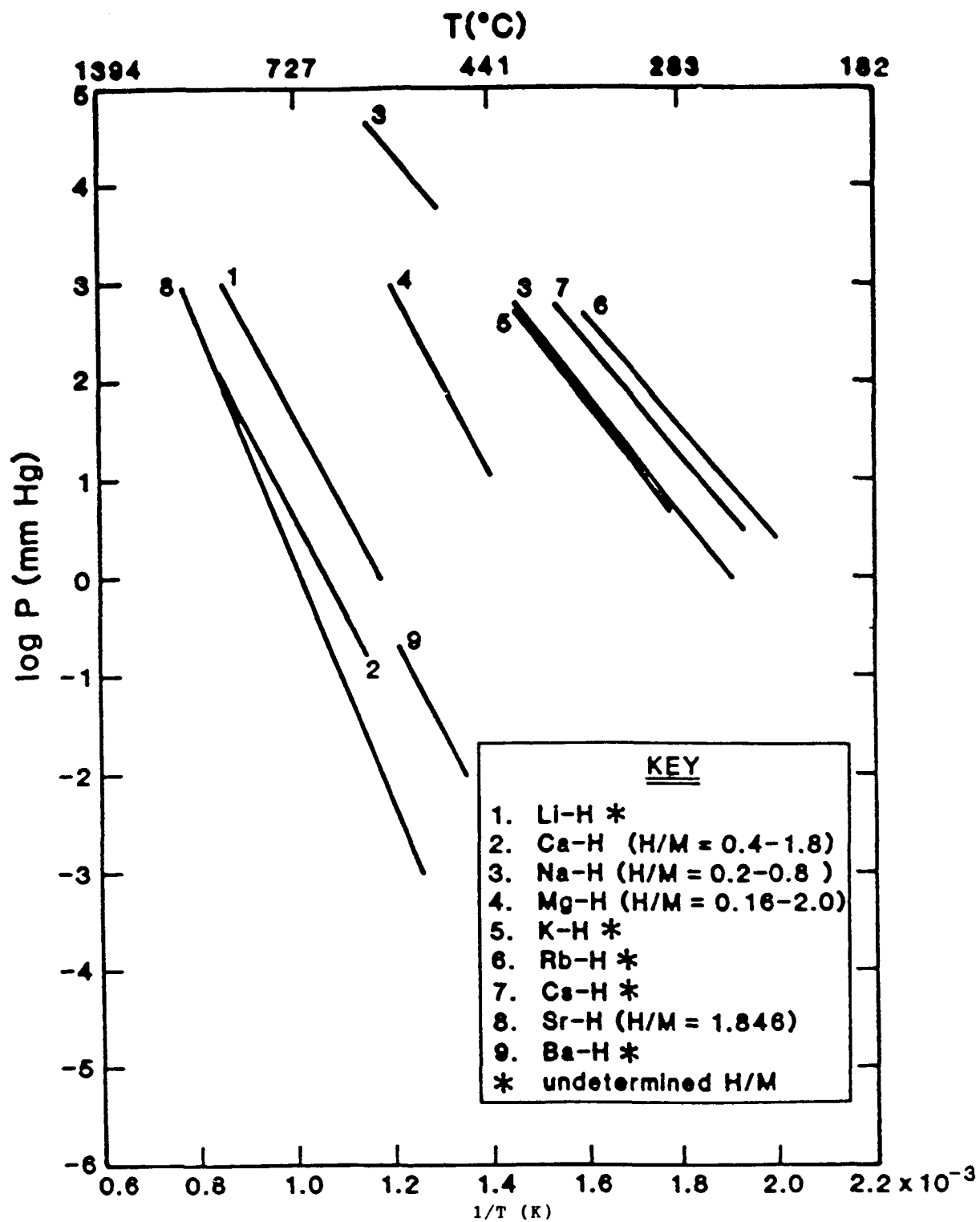


Fig. 6. Van't Hoff curves for the saline hydrides.

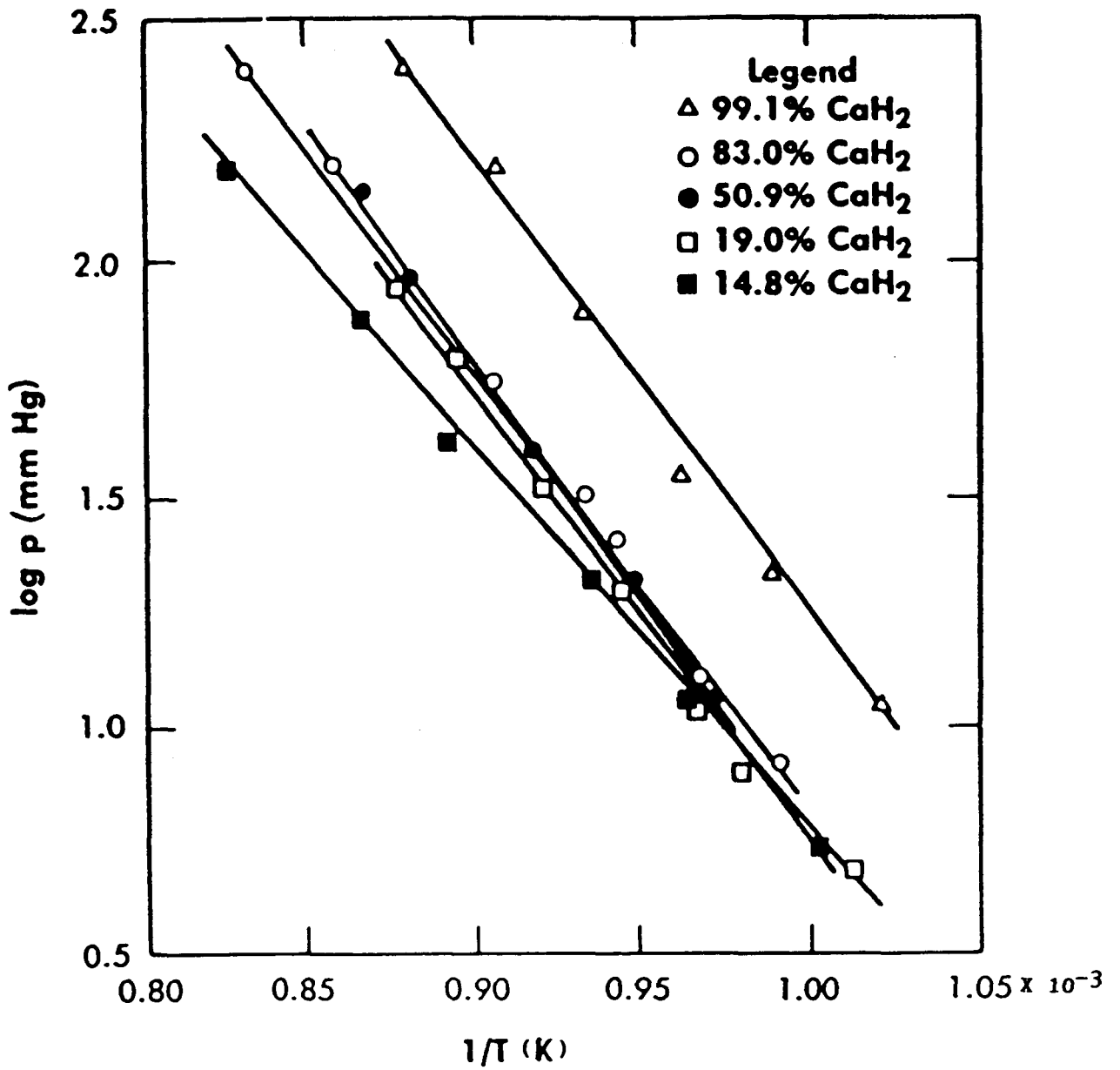


Fig. 7. Pressure-temperature isochores for the calcium-hydrogen system.

B. Group III A and IV A Hydrides

This section discusses the hydrides of zirconium, hafnium, titanium, yttrium, and scandium. Zirconium and hafnium hydrides are treated together, as are yttrium and scandium, whereas titanium is examined separately. Table II lists all of the van't Hoff constants for these hydrides; Fig. 8 plots the van't Hoff curves.

1. Zirconium and Hafnium Hydrides. Zirconium and hafnium are almost always found together as ores. Furthermore, they have similar chemical properties, and so it is not surprising that they form hydrides with similar properties.

Zirconium hydride's high number of hydrogen atoms per cubic centimeter (7×10^{22} , compared with 6.7×10^{22} for cold water) makes it an attractive hydrogen storage material.

In 1929 Hagg¹⁰ began work on the Zr-H system. Martin and Rees¹¹ developed a lattice model with hydrogen-occupied interstitial sites for the Zr-H system in 1954. The number of hydrogen-occupied sites decreases with increasing temperature, thus accounting for decreasing adsorption. This is evident in Fig. 9, which is a composite graph from the work of four investigators, as the plateaus disappear dramatically between 850°C and 900°C. Figure 10 is a complete pressure-temperature isochore graph, from 4 to 66 at.% hydrogen, summarizing the work of Ells and McQuillan¹⁶ and Gulbransen and Andrew.¹⁵ The van't Hoff data for the Zr-H system were constructed from Fig. 9 at H/M = 1.0.

Adding other elements to zirconium causes various effects. Oxygen tends to stabilize the phases of the Zr-H systems. The alloying of other metals to zirconium raises plateau pressures, except with scandium¹⁷ (see Fig. 11). Only the addition of nickel leads to a substantial increase in hydrogen content.¹⁸

TABLE II

GROUP III A AND GROUP IV A HYDRIDES VAN'T HOFF CONSTANTS

<u>System</u>	<u>A</u>	<u>B</u>	<u>Temperature Range</u> <u>(°C)</u>
Zr-H	11216.7	12.5902	500-850
Hf-H	6251.05	7.7147	683-872
Y-H	9709.0	8.80	600-950
	11869.0	10.52	900-1350
Sc-H	9050.0	9.17	800-1100
Ti-H	8573.7	12.26	427-636

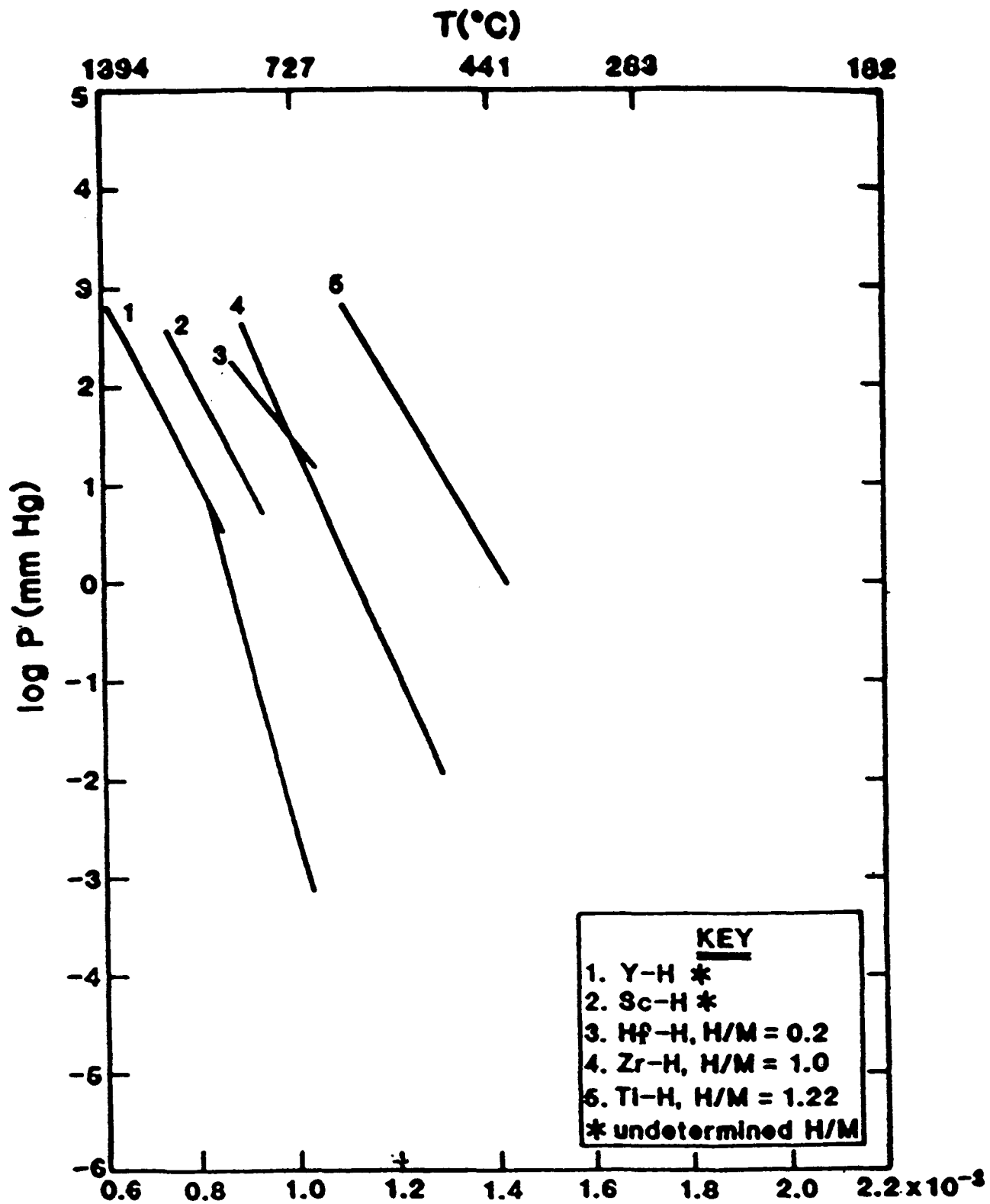


Fig. 8. Van't Hoff curves for Group III A and IV A hydrides.

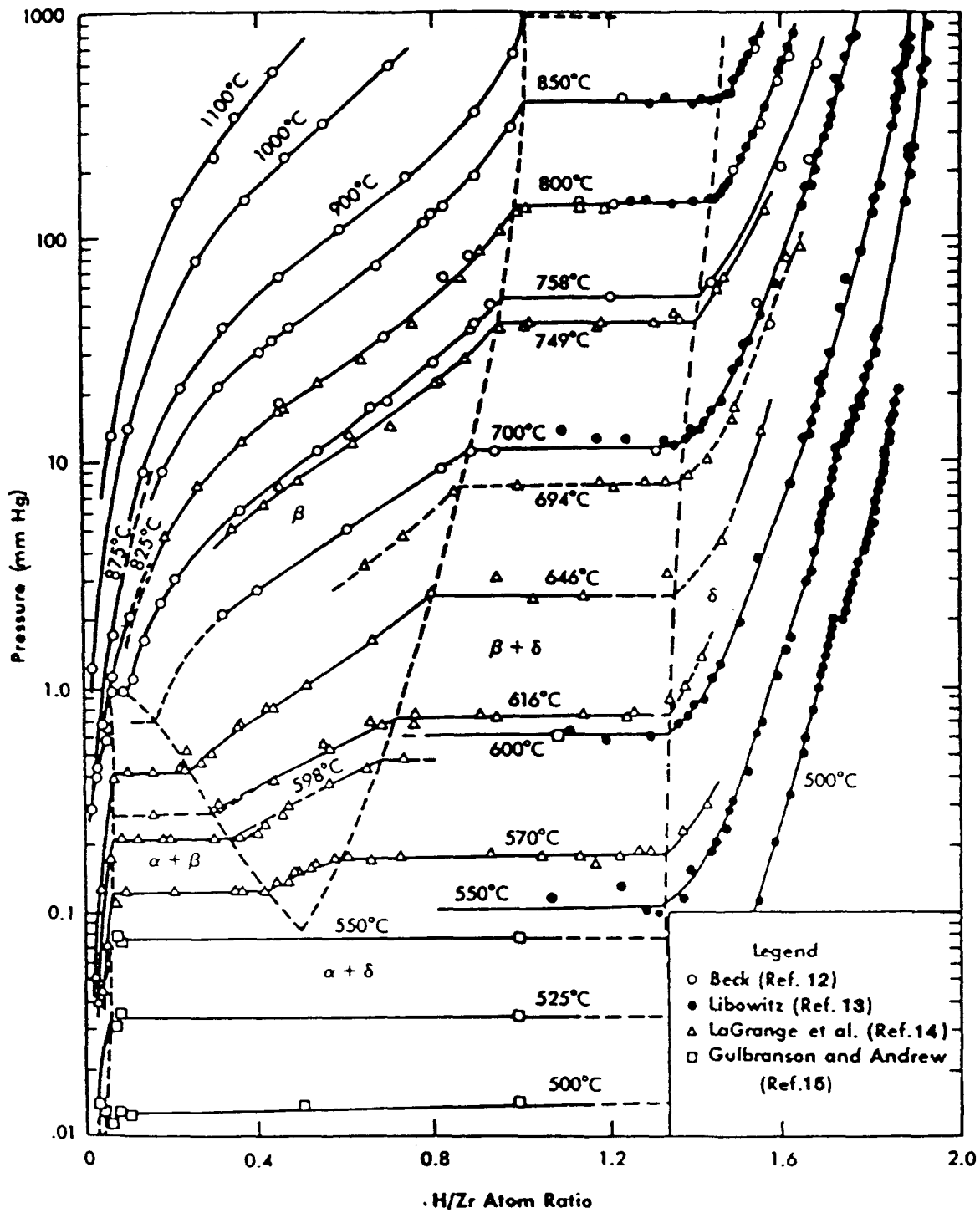


Fig. 9. Pressure-composition isotherms for the zirconium-hydrogen system.

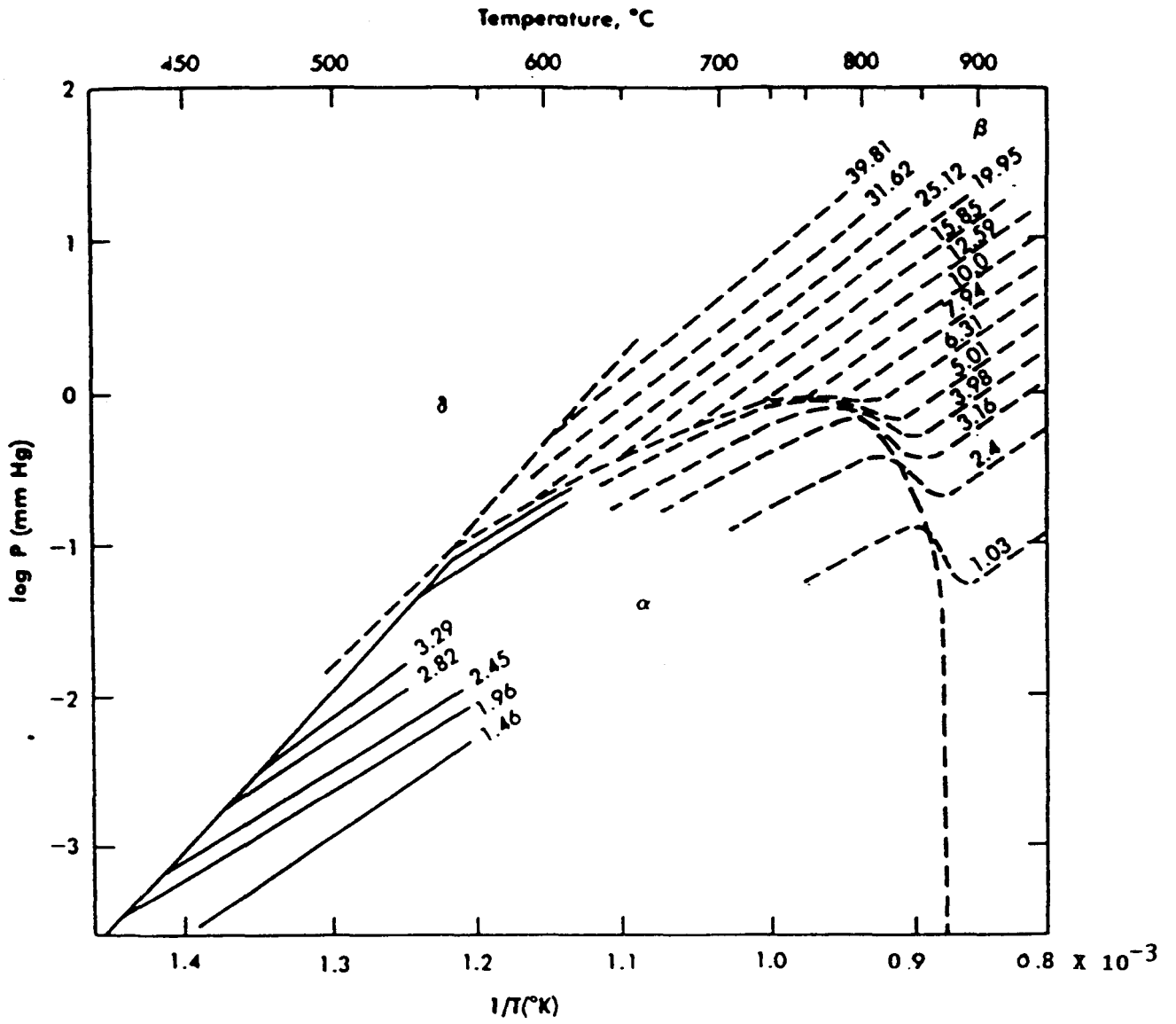


Fig. 10. Pressure-temperature isochores for the zirconium-hydrogen system.

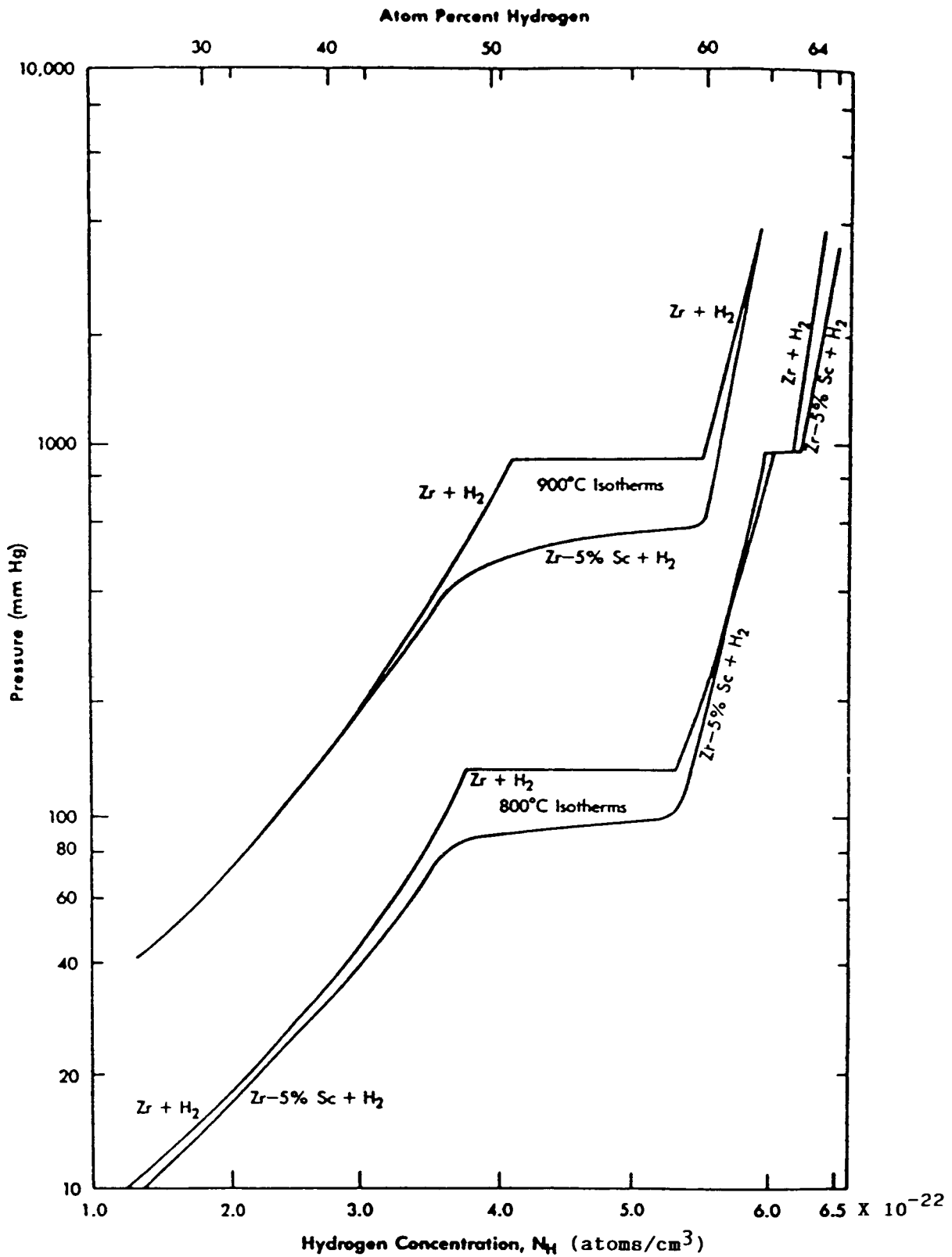


Fig. 11. Pressure-composition isotherms comparing the zirconium-scandium-hydrogen system with the zirconium-hydrogen system.

Researchers have not investigated hafnium hydride as extensively as zirconium hydride. Indeed, Edwards and Veleckis¹⁹ report the only available PCT data, Fig. 12. The pressure plateaus are all less than 200 mm Hg, considerably lower than those of the Zr-H system. Also, the plateaus end much more abruptly than in the Zr-H system. The van't Hoff equation for the Hf-H system was constructed from Fig. 9 at $H/M = 2$.

2. Titanium Hydrides. Titanium exhibits a high solubility for hydrogen and a relatively low molecular weight, both desirable characteristics of a gettering system. These two properties combine to give titanium a high hydrogen density, well above that of cold water. Beck's¹⁷ experiments produced data that agreed with data of previous investigators. Figures 13 and 14 summarize his findings. Gibb and Kruschwitz²⁰ found that nitrogen and oxygen impurities would occupy interstitial sites, thus reducing the hydrogen content of the getter.

The van't Hoff equation for the Ti-H system was derived from the data in Fig. 13 at 2.5 wt% hydrogen.

3. Yttrium and Scandium Hydrides. Figures 15 and 16 are PCT data for the Y-H system. Lundun and Blackledge²¹ studied the system from 900°C to 1350°C, whereas Yannopoulos, Edwards, and Wahlbeck²² investigated from 601.4°C to 949.4°C. The pressure plateaus start at a H/M ratio of 0.6 and continue up to 0.9 through 1.6, depending on the pressure and temperature.

Figure 17 shows the Sc-H system from the work of Lieberman and Wahlbeck.¹ The hysteresis is negligible for the range of pressures and temperatures studied.

Van't Hoff equations for both the Y-H and the Sc-H systems are the work of their respective investigators.

C. Rare-Earth Hydrides

The rare-earth hydrides are the hydrides of the lanthanide series (atomic numbers 57 to 71). They are characterized by their electronic structure; the 4f shell is filled before the 5d level. All rare-earth metals, with the exception of cerium, have high thermal-neutron absorption cross sections, a property that is used for reactor shielding and control methods. All rare earths (except europium and ytterbium) form dihydrides and can easily accommodate more hydrogen to form trihydrides. Korst and Warf²³ have studied the rare-earth hydrides extensively.

Figure 18 is a plot of the rare-earth hydride van't Hoff curves, and Table III gives the van't Hoff constants used to construct these curves. Figure 19 is the expanded van't Hoff curves for rare-earth hydrides.

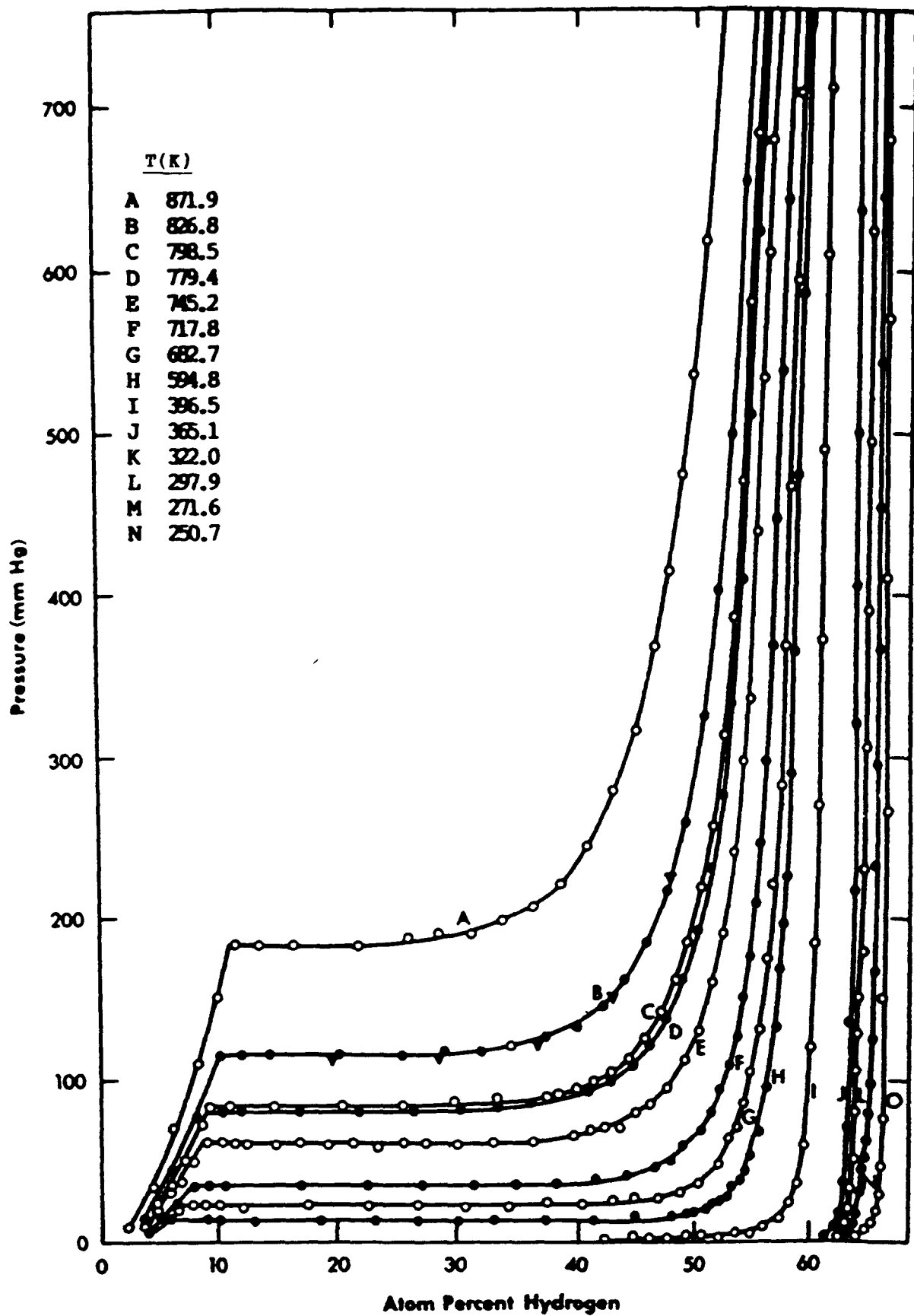


Fig. 12. Pressure-composition isotherms for the hafnium-hydrogen system.

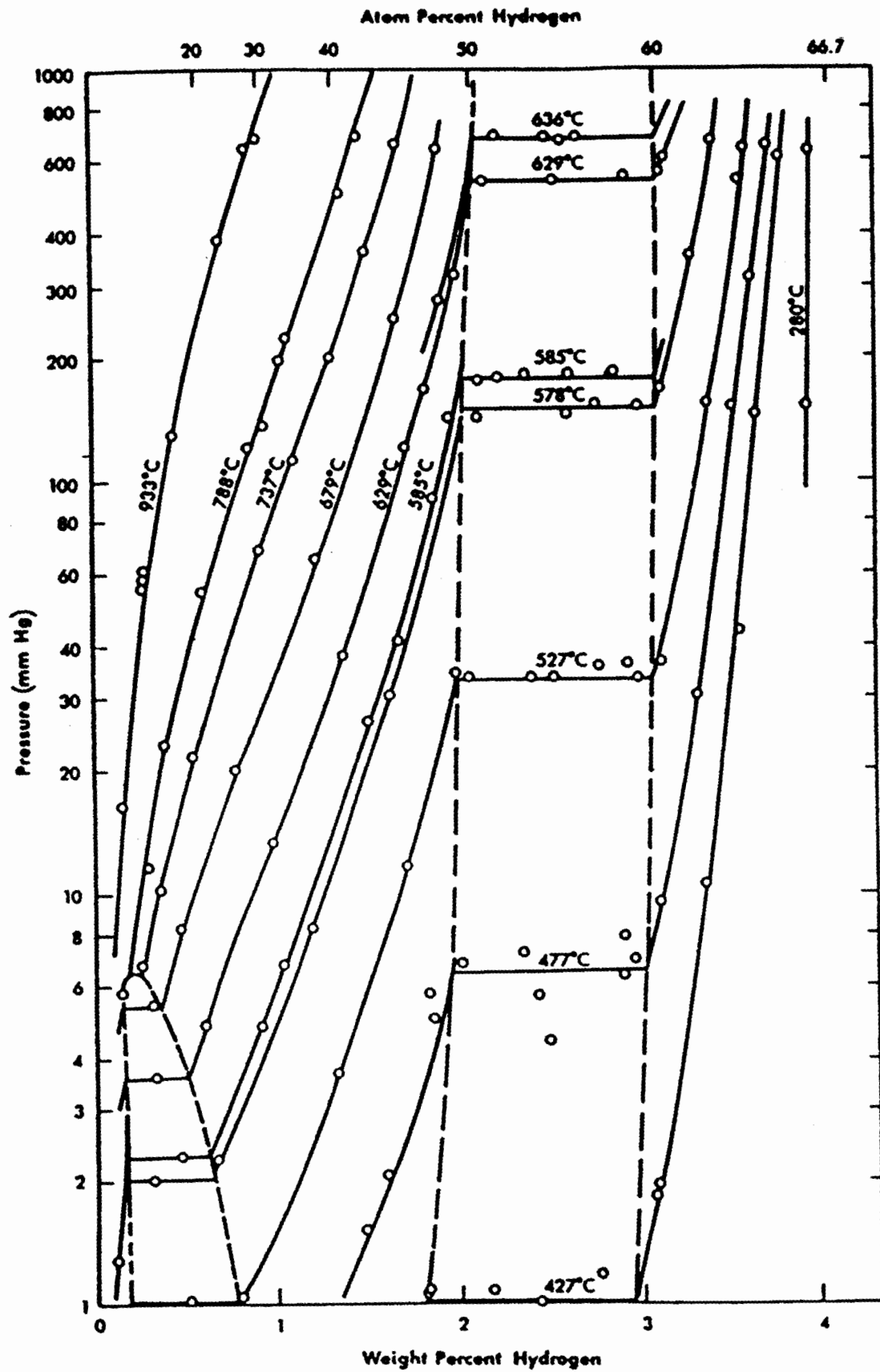


Fig. 13. Pressure-composition isotherms for the titanium-hydrogen system.

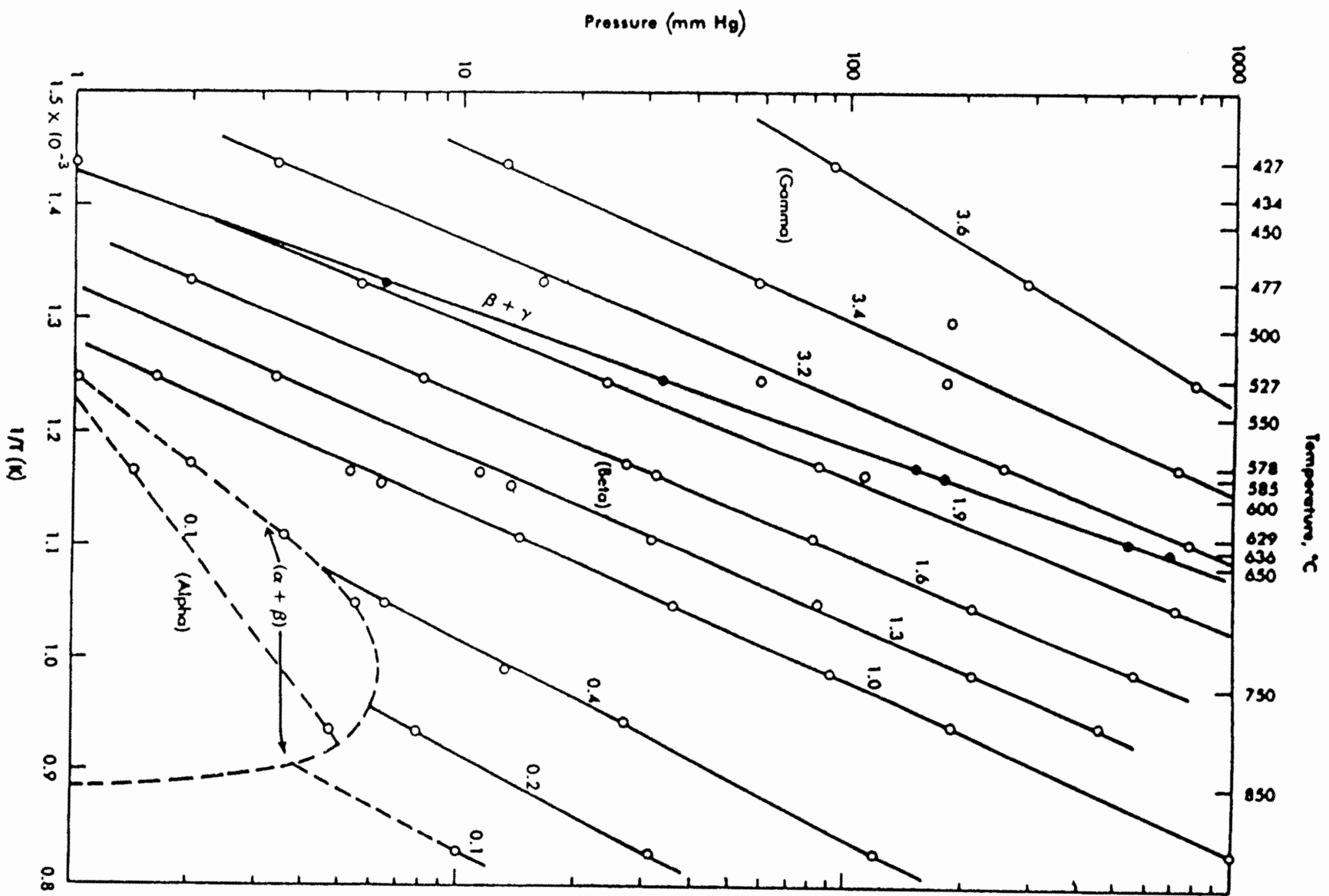


FIG. 14. Pressure-temperature isochores for the titanium-hydrogen system.

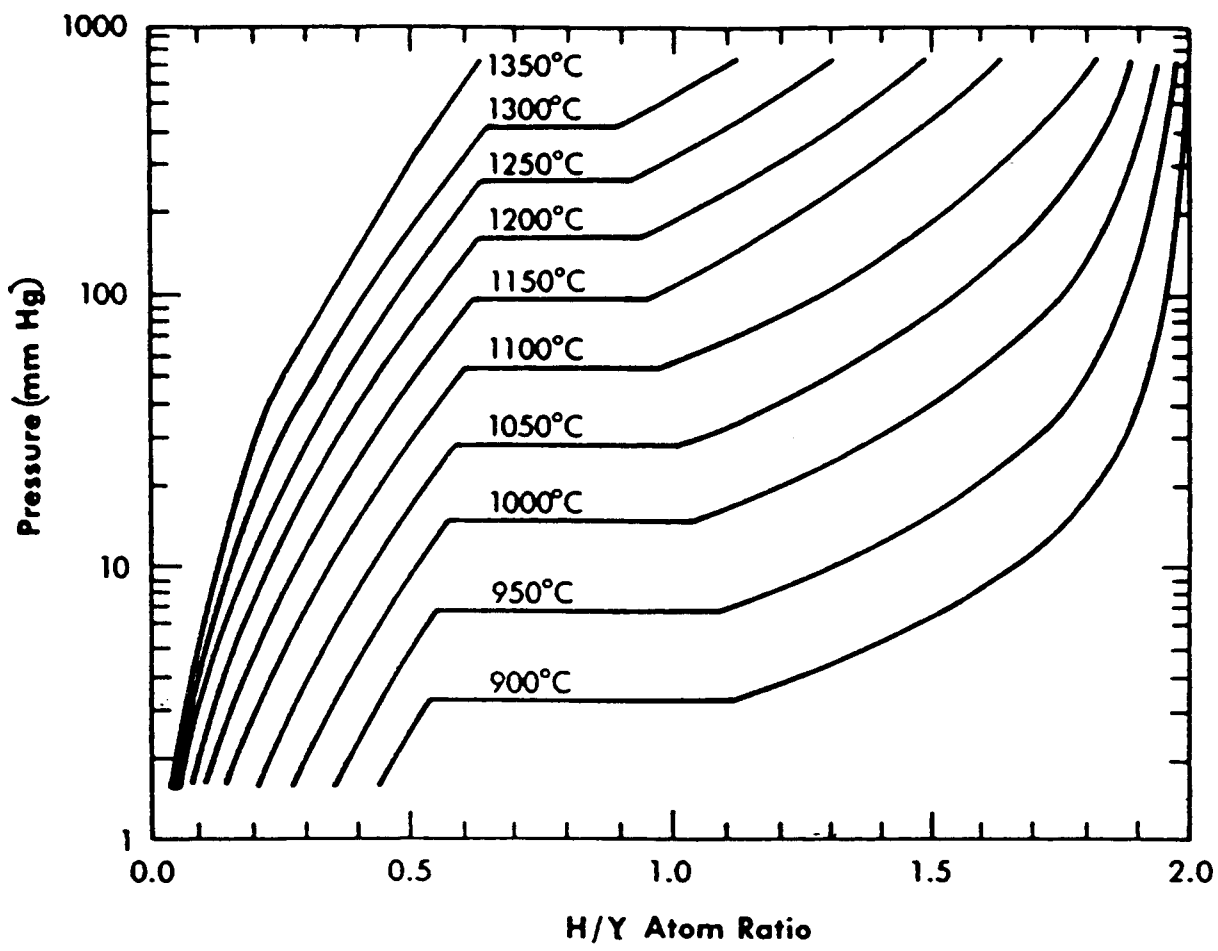


Fig. 15. Pressure-composition isotherms for the yttrium-hydrogen system.

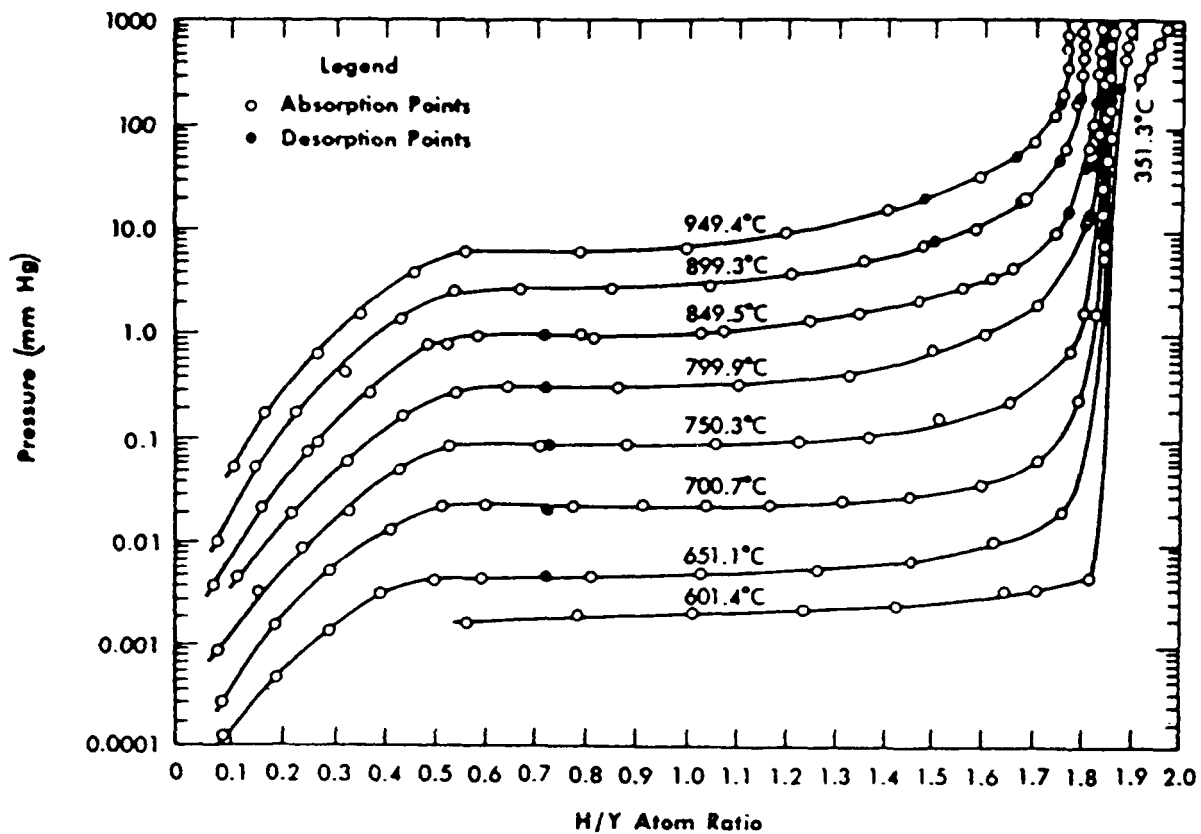


Fig. 16. Pressure-composition isotherms for the yttrium-hydrogen system.

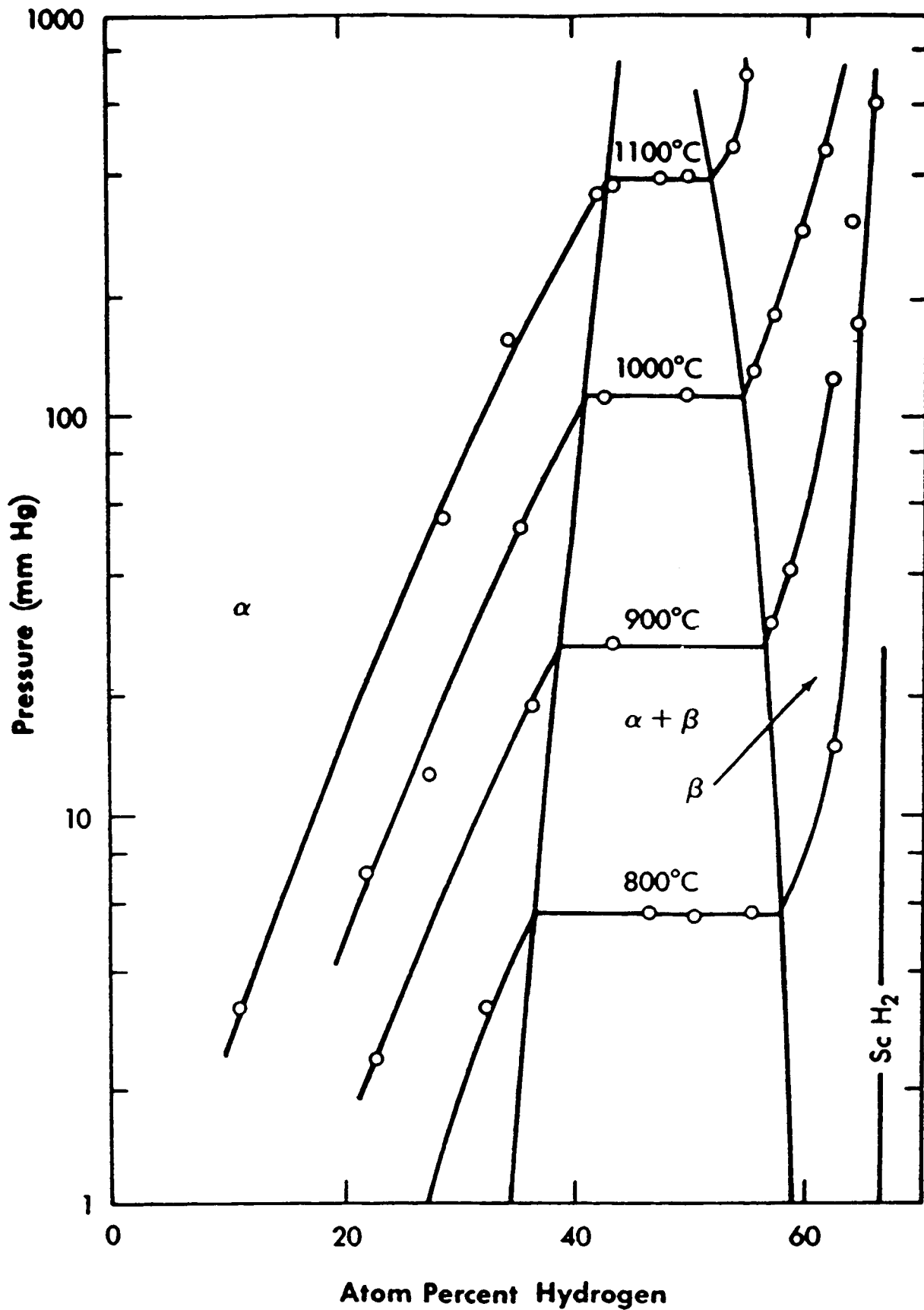


Fig. 17. Pressure-composition isotherms for the scandium-hydrogen system.

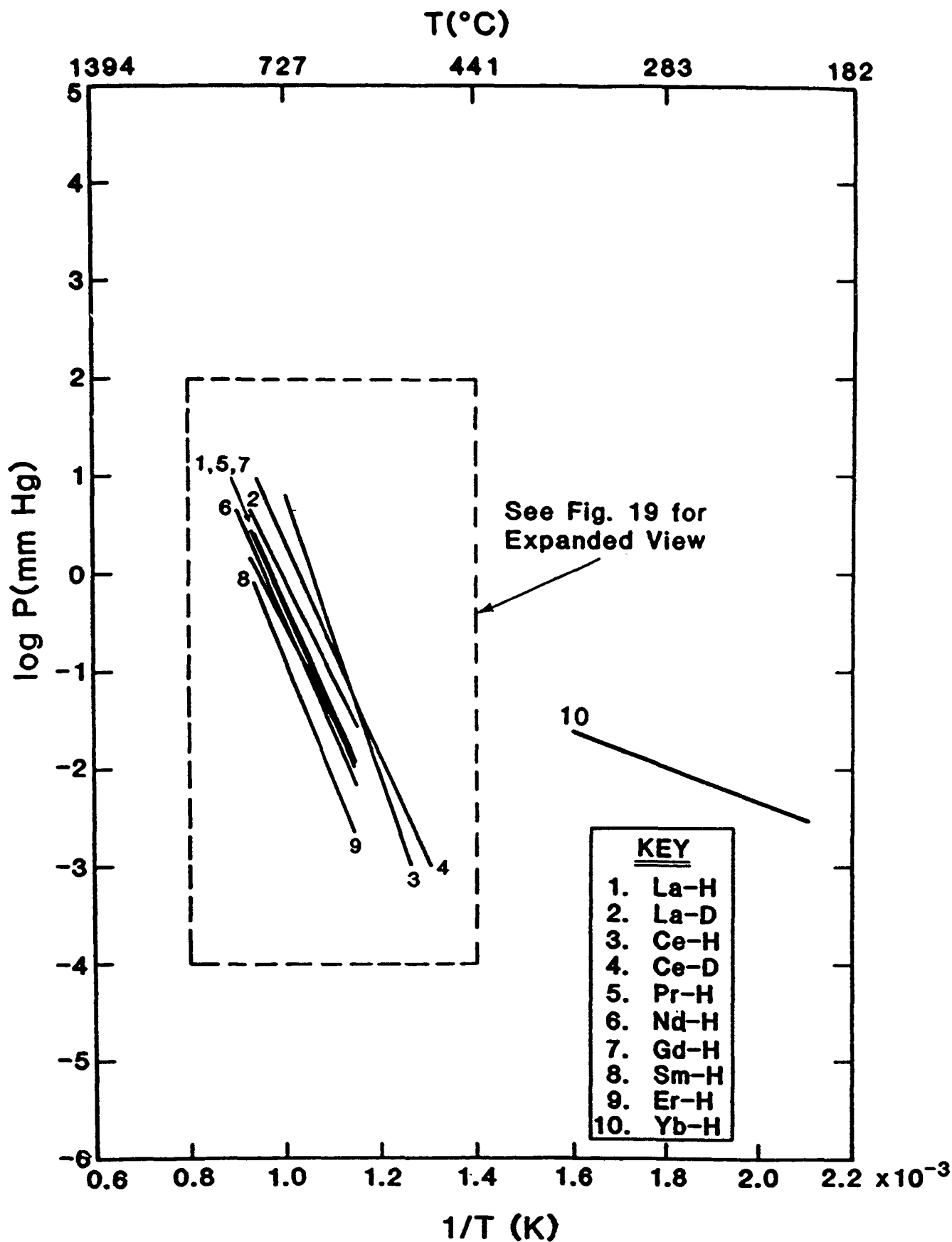


Fig. 18. Van't Hoff curves for the rare-earth hydrides.

TABLE III
RARE-EARTH HYDRIDES VAN'T HOFF CONSTANTS

<u>System</u>	<u>A</u>	<u>B</u>	<u>Temperature Range (°C)</u>
La-H	10847	10.644	598-798
La-D	10173	10.107	598-798
Ce-H	10761	10.63	516-670
Ce-D	10123	10.205	493-800
Pr-H	10879	10.526	600-800
Nd-H	11031	10.482	600-839
Sm-H	11700	10.526	600-800
Gd-H	10250	9.72	600-800
Er-H	11900	11.0	600-800
Yb-H	1440	65.92	200-352

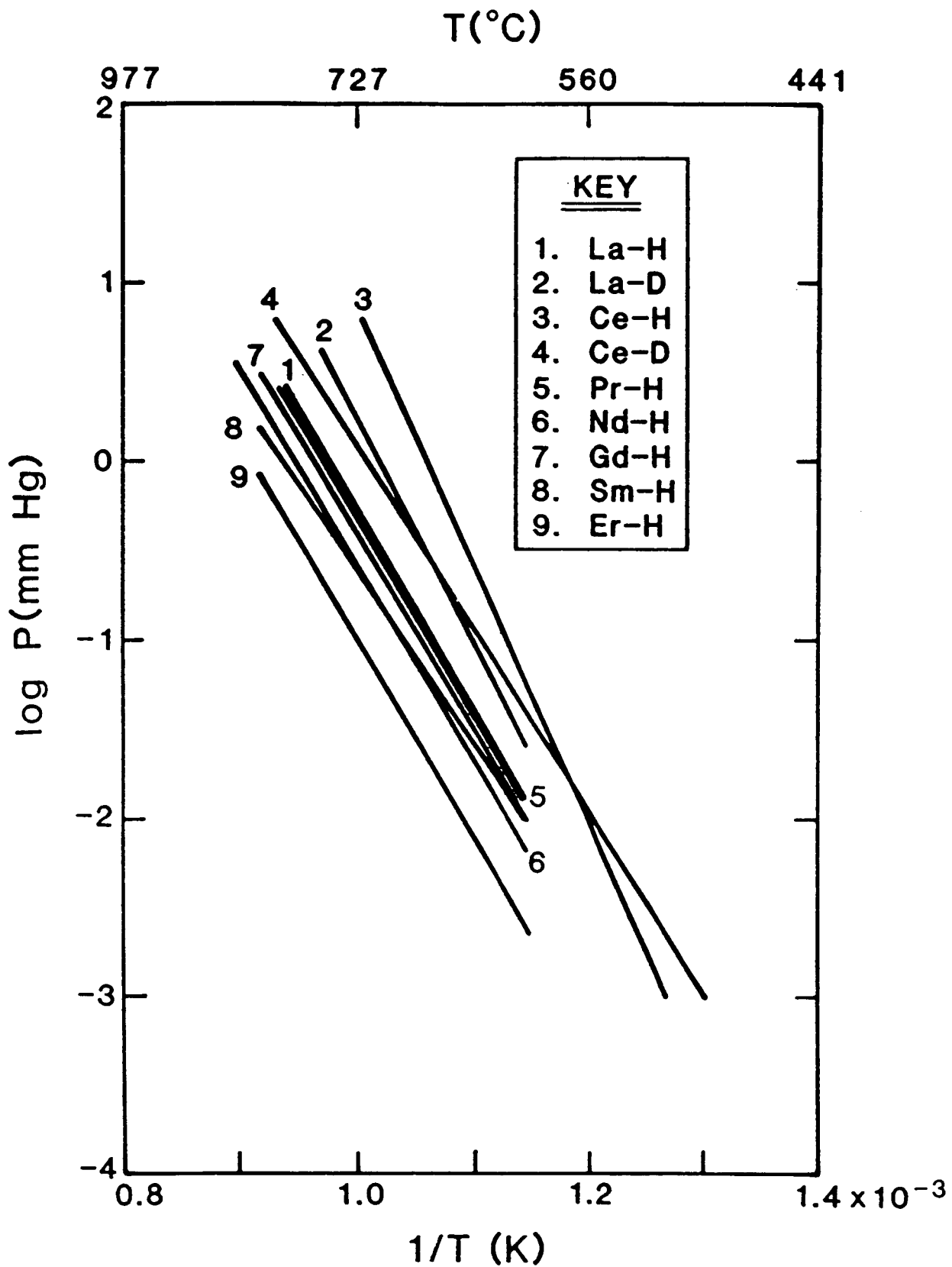


Fig. 19. Expanded van't Hoff curves for rare-earth hydrides.

Korst and Warf²³ thoroughly investigated lanthanum hydride up to atmospheric pressure; Figs. 20 and 21 show their results. They detected no hysteresis within experimental error. They also encountered higher equilibrium pressures when working with deuterium, as was expected.

Korst and Warf²³ also investigated the Ce-H system at higher pressures (up to 40 atm), as seen in Fig. 22. The van't Hoff constants given in Table III were determined at plateau-pressure compositions, including data for the Ce-D system.

Praseodymium PCT data were not reliably reproduced at low pressures, but van't Hoff curves using the data of Korst and Warf²³ (Fig. 23) are probably the most accurate.

Figure 24 shows the results of Korst and Warf²³ and Mulford and Holley²⁴ from their work with the Nd-H system. They reached fairly good agreement in the plateau region, but the single-phase region was not reproducible. Again, the van't Hoff constants of Korst and Warf²³ were used.

The Sm-H system has not been studied extensively. Figure 25 is an isotherm at 600°C for the Sm-D system as reported by Korst and Warf.²³

Sturdy and Mulford²⁵ used higher-purity gadolinium than that available to earlier investigators and thereby obtained an accurate representation of the Gd-H system. Figures 26 and 27, which show their results, illustrate the two constant pressure plateaus of the Gd-H system. The investigators also reported the van't Hoff constants for this system.

TABLE III
RARE-EARTH HYDRIDES VAN'T HOFF CONSTANTS

System	A	B	Temperature Range (°C)
La-H	10847	10.644	598-798
La-D	10173	10.107	598-798
Ce-H	10761	10.63	516-670
Ce-D	10123	10.205	493-800
Pr-H	10879	10.526	600-800
Nd-H	11031	10.482	600-839
Sm-H	11700	10.526	600-800
Gd-H	10250	9.72	600-800
Er-H	11900	11.0	600-800
Yb-H	1440	65.92	200-352

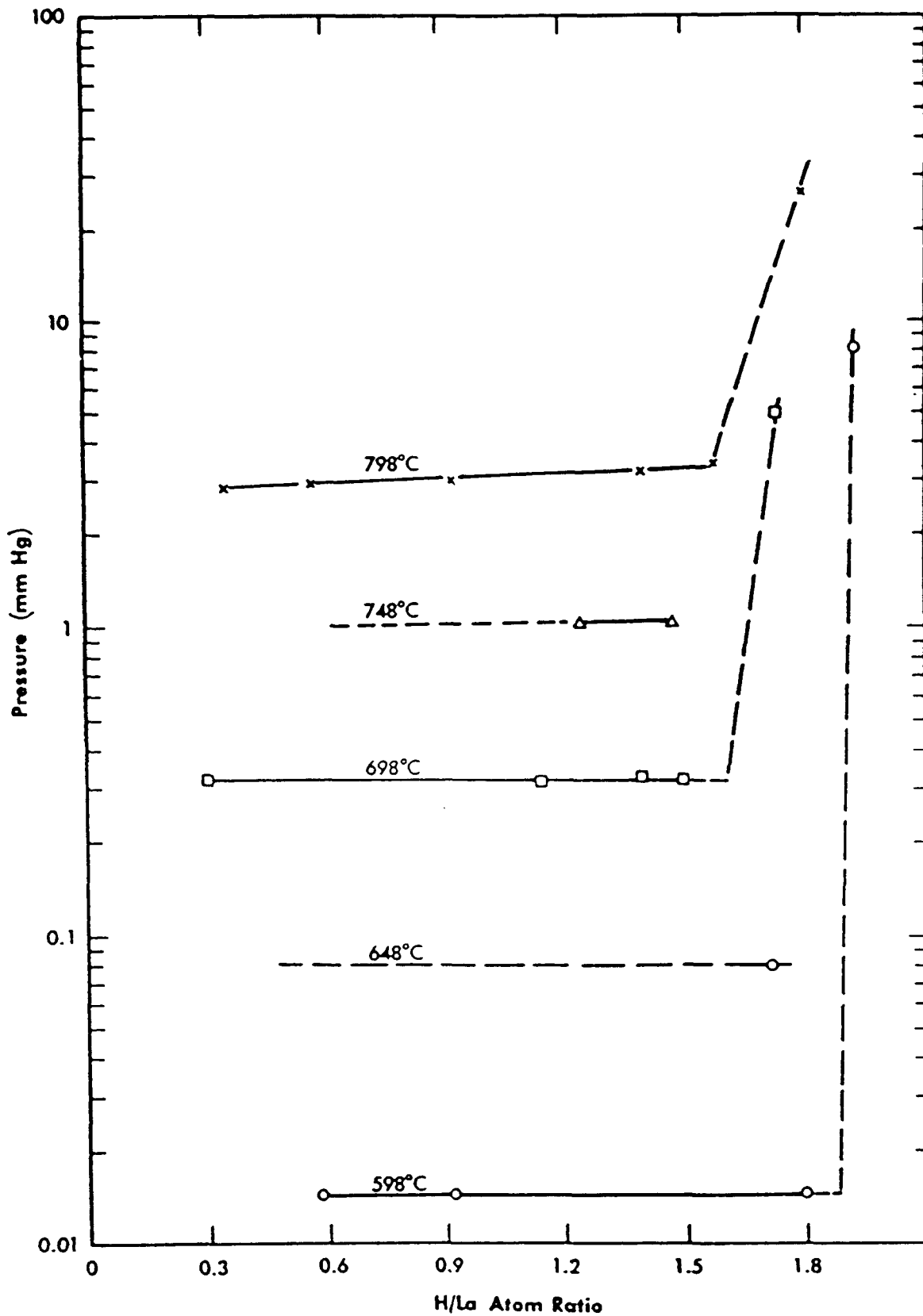


Fig. 20. Pressure-composition isotherms for the lanthanum-hydrogen system.

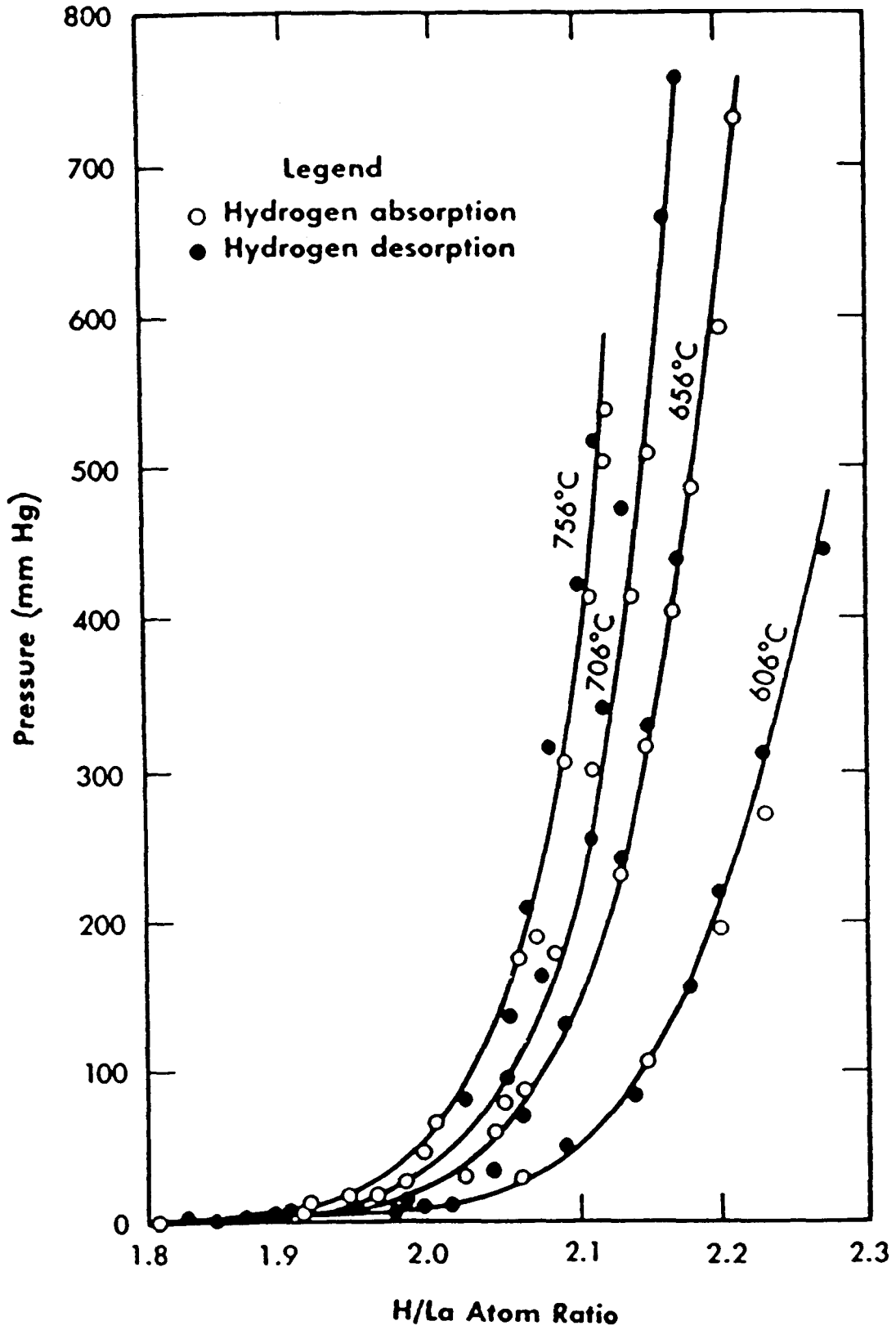


Fig. 21. Pressure-composition isotherms for the lanthanum-hydrogen system.

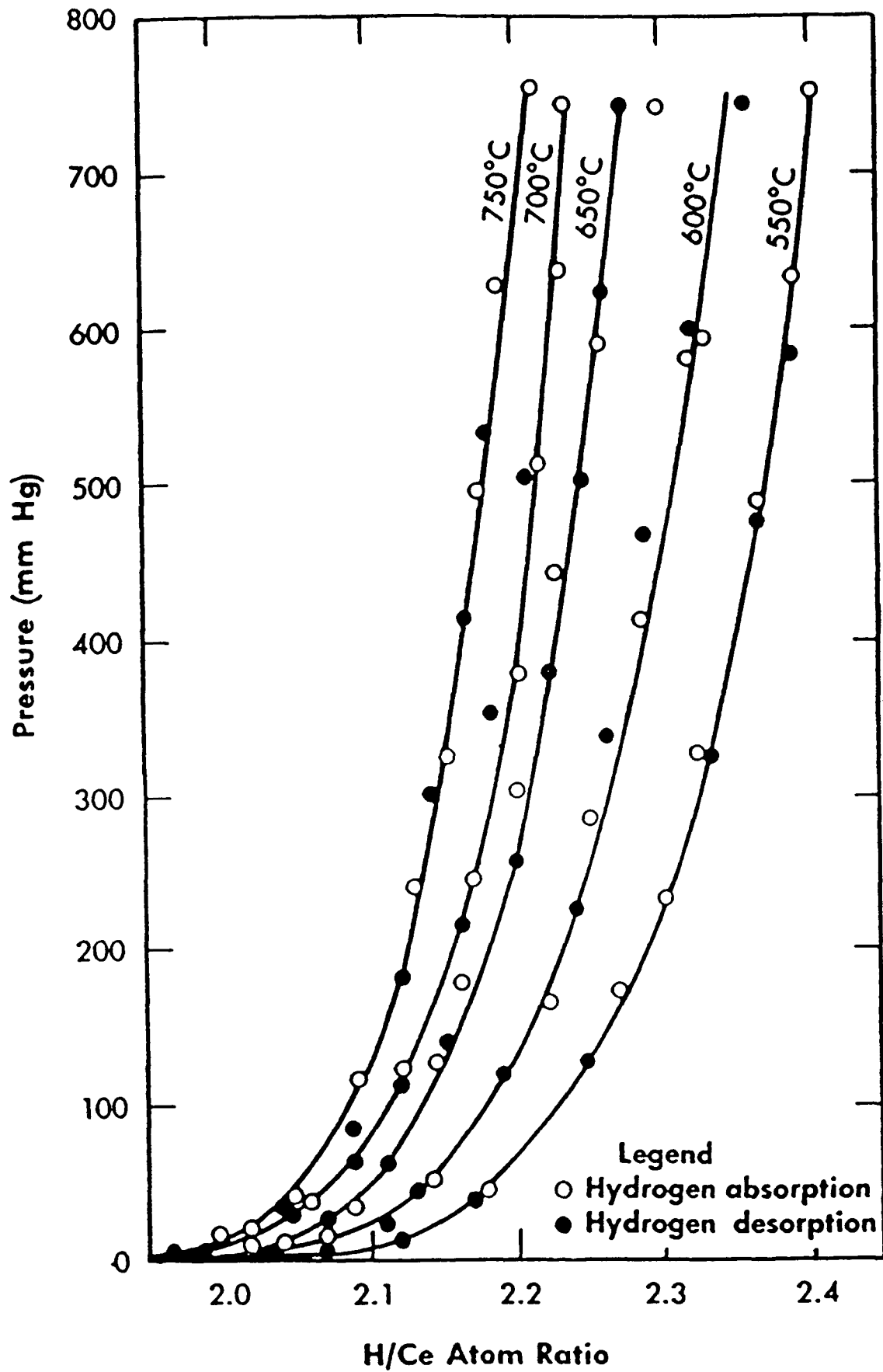


Fig. 22. Pressure-composition isotherms for the cerium-hydrogen system.

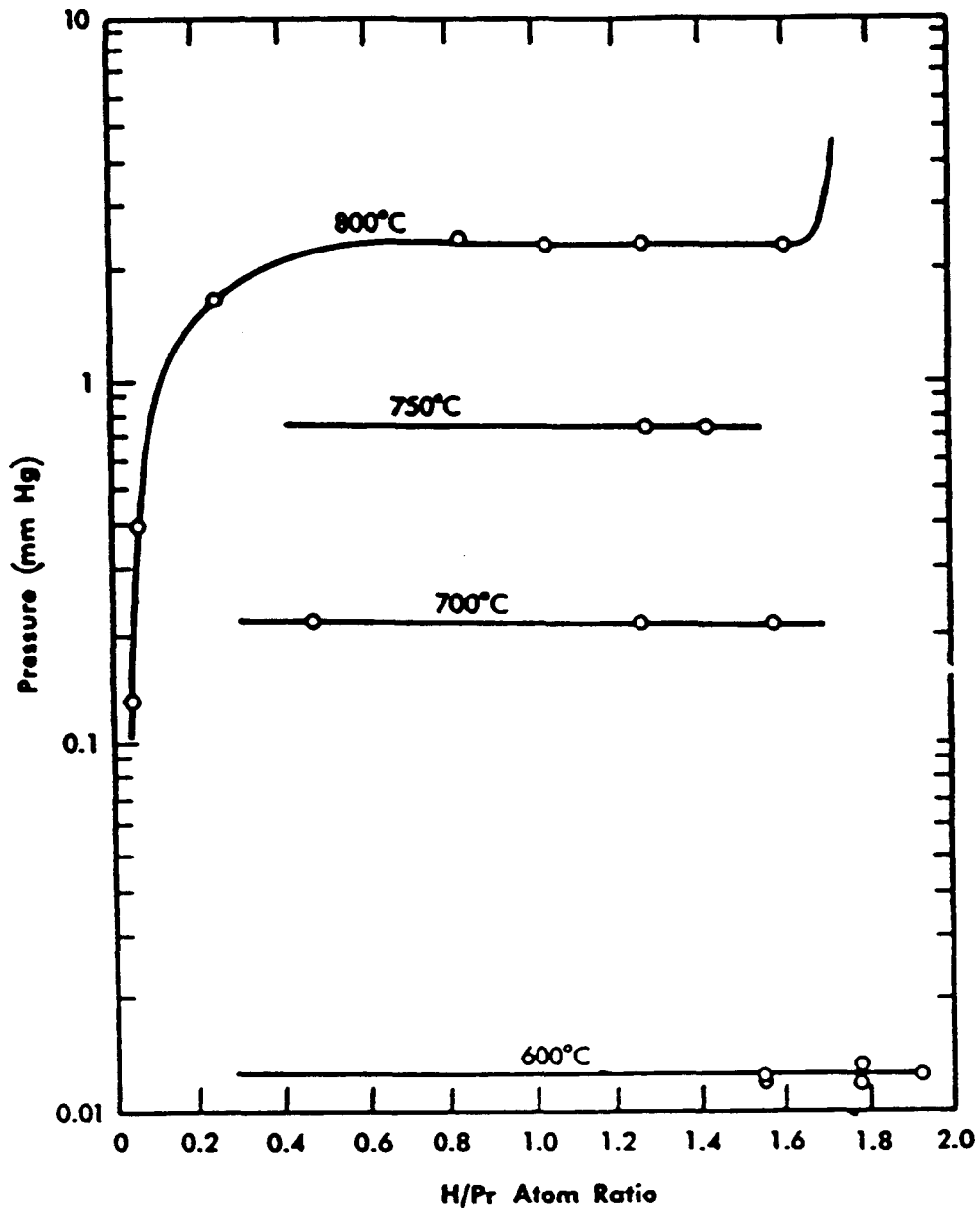


Fig. 23. Pressure-composition isotherms for the praseodymium-hydrogen system.

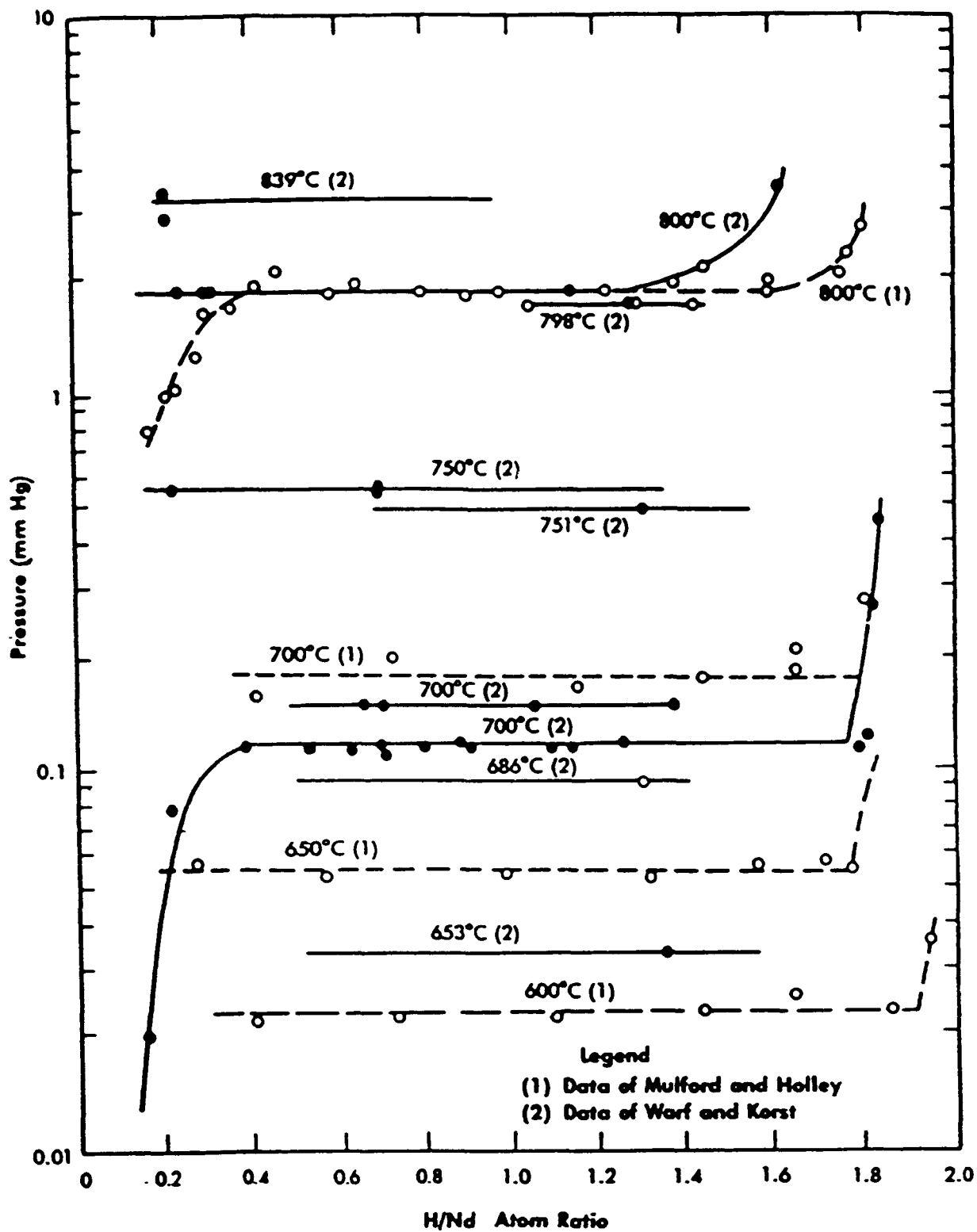


Fig. 24. Pressure-composition isotherms for the neodymium-hydrogen system.

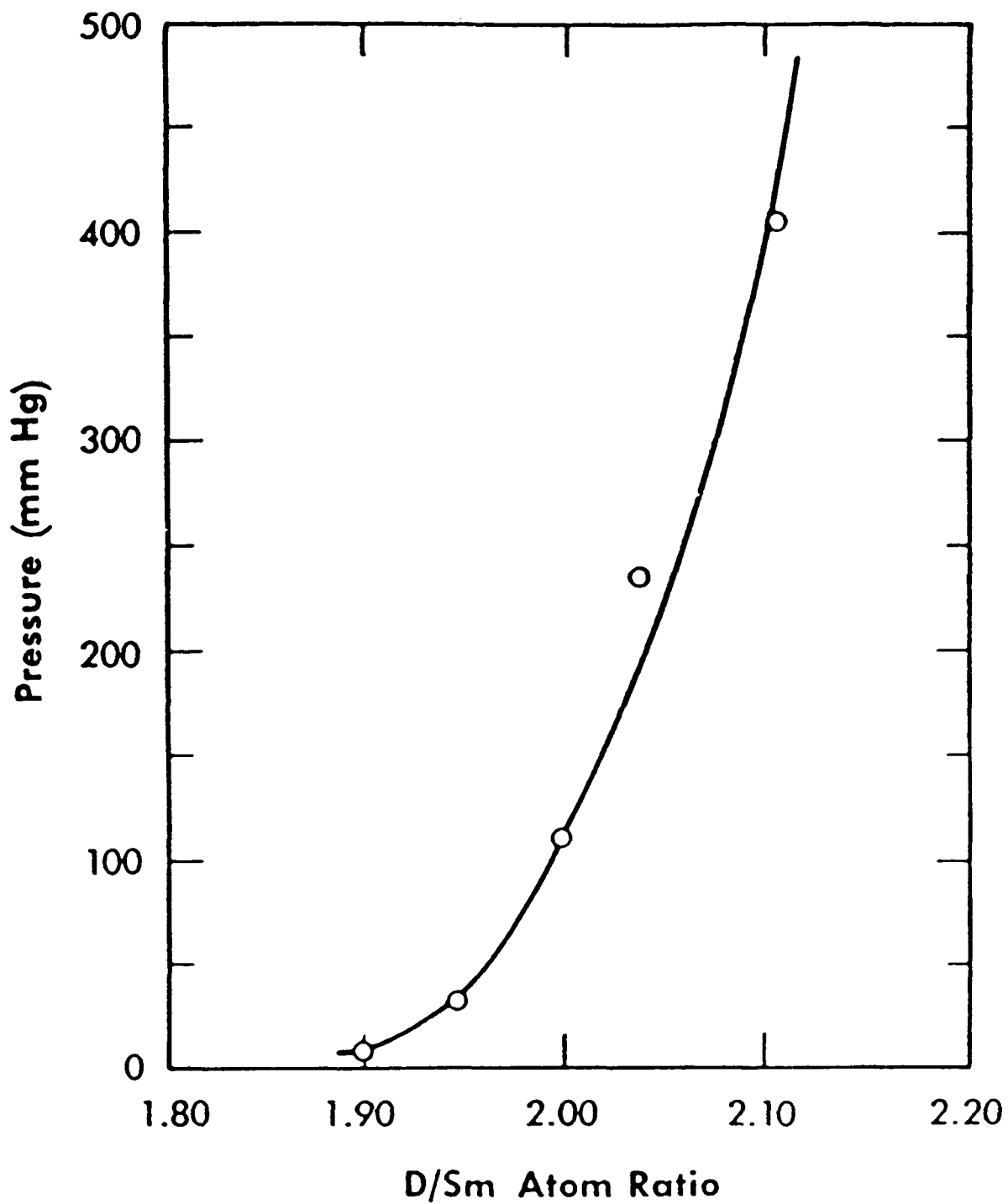


Fig. 25. Pressure-composition isotherm (600°C) for the samarium-deuterium system.

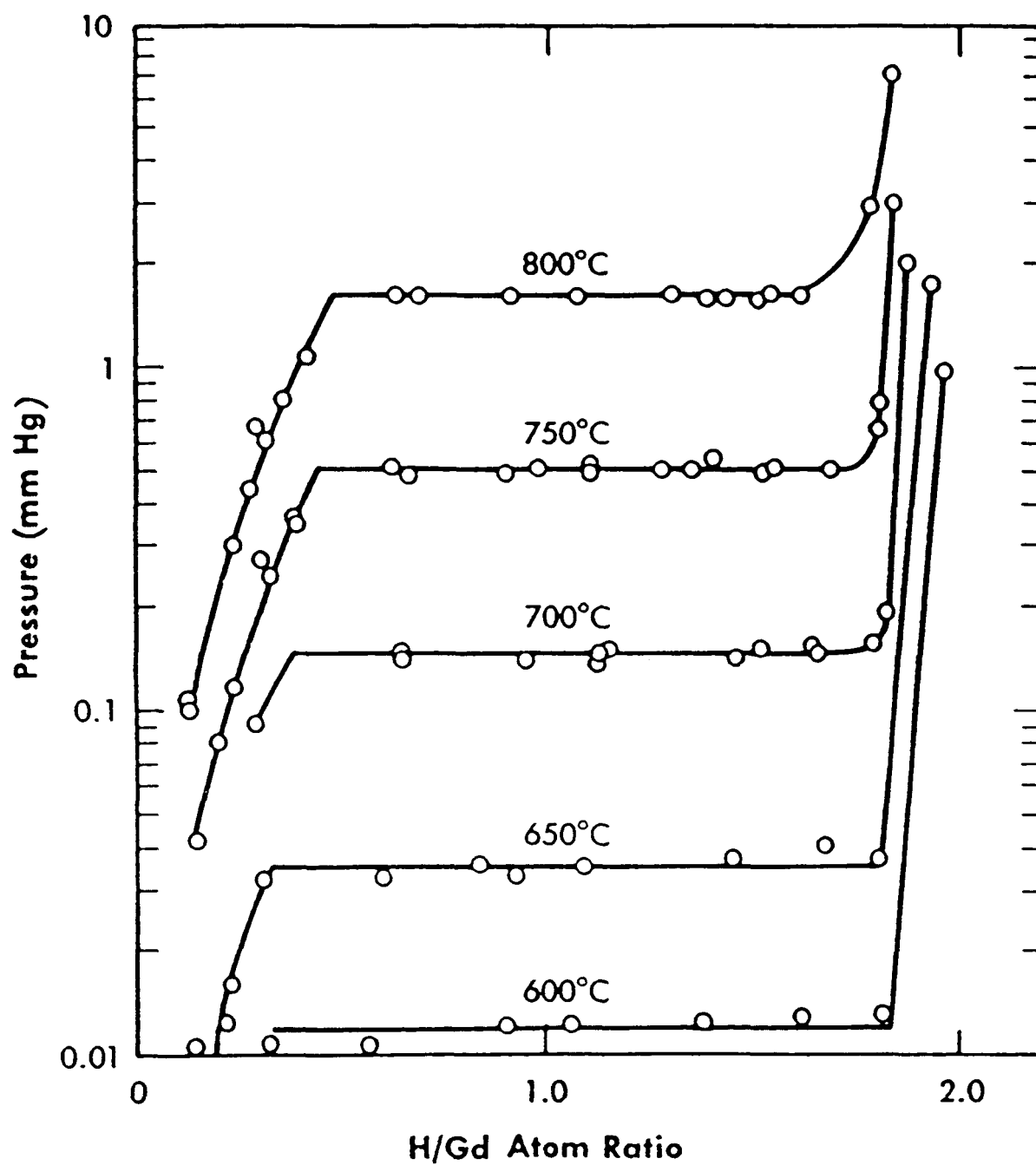


Fig. 26. Pressure-composition isotherms for the gadolinium-hydrogen system.

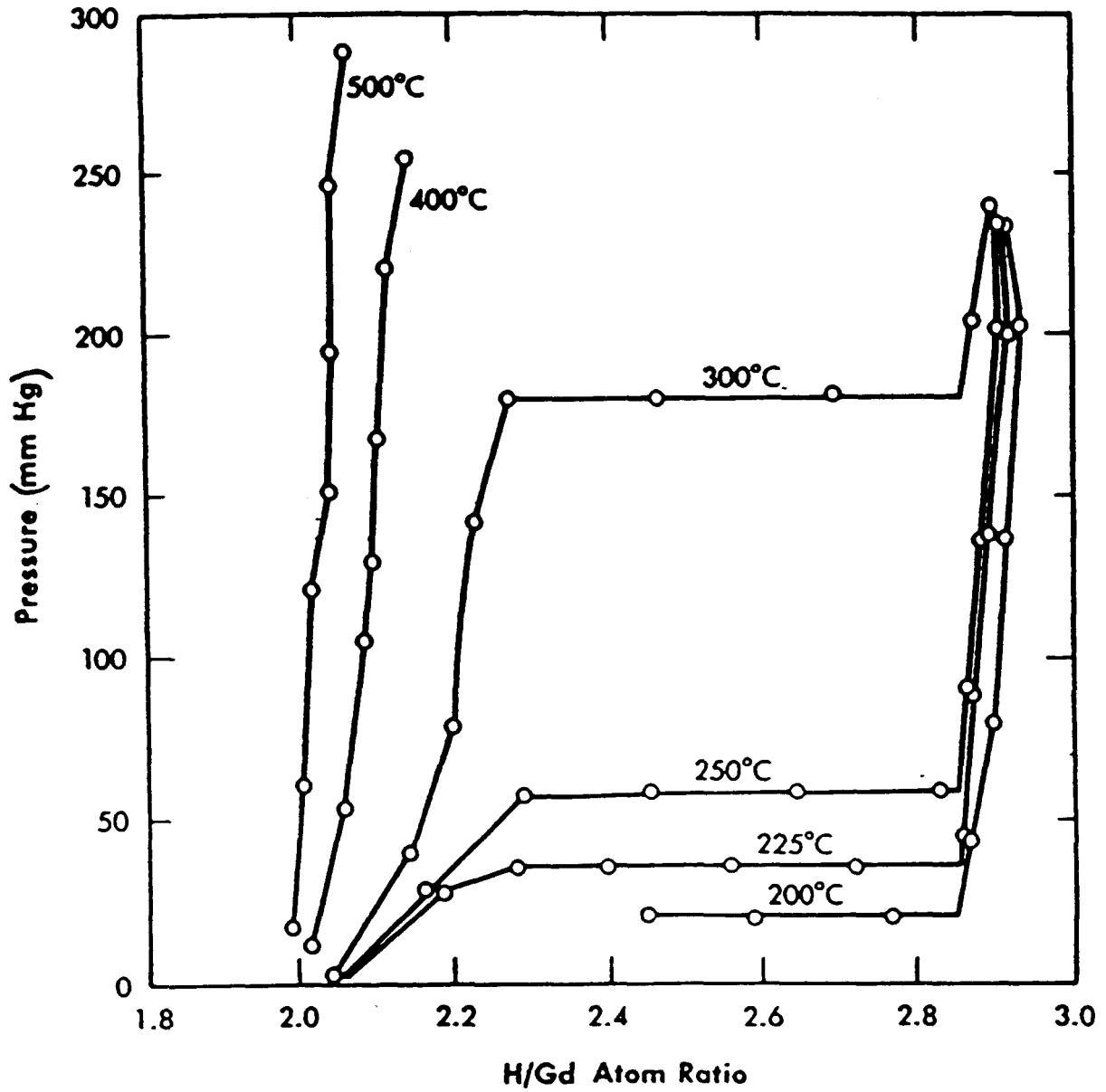


Fig. 27. Pressure-composition isotherms for the gadolinium-hydrogen system.

Mulford²⁶ investigated erbium hydride and reported its van't Hoff constants. No other dissociation pressure or thermodynamic data are available.

The Warf and Hardcastle²⁷ PCT data for the Yb-H system are shown in Fig. 28. Table III gives the van't Hoff constants for the plateau regions of these curves.

D. Actinide Hydrides

The actinide elements are extremely important in nuclear technology because uranium, thorium, and plutonium are used as fuels. Moreover, because hydrogen is an efficient moderator, the equilibrium relationships between these elements and hydrogen must be understood to safely apply these actinides in a nuclear environment.

As do the lanthanide elements, the actinides fill an underlying electron shell when they react chemically. However, the actinides do not have as similar properties as do the lanthanides.

Dissociation pressure and thermodynamic data concerning the actinide hydrides are sparse. The element that has been studied in depth for such information is uranium; little information is available on the Th-H, Pu-H, and Np-H systems.

Table IV lists uranium's van't Hoff constants, and Fig. 29 plots the corresponding van't Hoff equation for uranium hydride.

Uranium reacts with hydrogen in a wide range of temperatures. The reaction rate increases up to 225°C, then decreases. Rates are slower for deuterium, possibly because of higher activation energies. Figures 30 and 31 are PCT data for the U-H system obtained from Spedding et al.²⁸ and Wicke and Otto,²⁹ respectively. It is obvious that there is a large increase in hysteresis for a small increase in temperature. One of the main advantages of uranium is that it hydrides at room temperature. Also, tritium in an inert gas can be scavenged to a level less than 1 mCi/m³ with a uranium bed at 0°C (273 K).

TABLE IV
URANIUM HYDRIDE VAN'T HOFF CONSTANTS

<u>System</u>	<u>A</u>	<u>B</u>	<u>Temperature Range</u> <u>(°C)</u>
U-H	4500	9.28	260-430
	4410	9.14	450-650

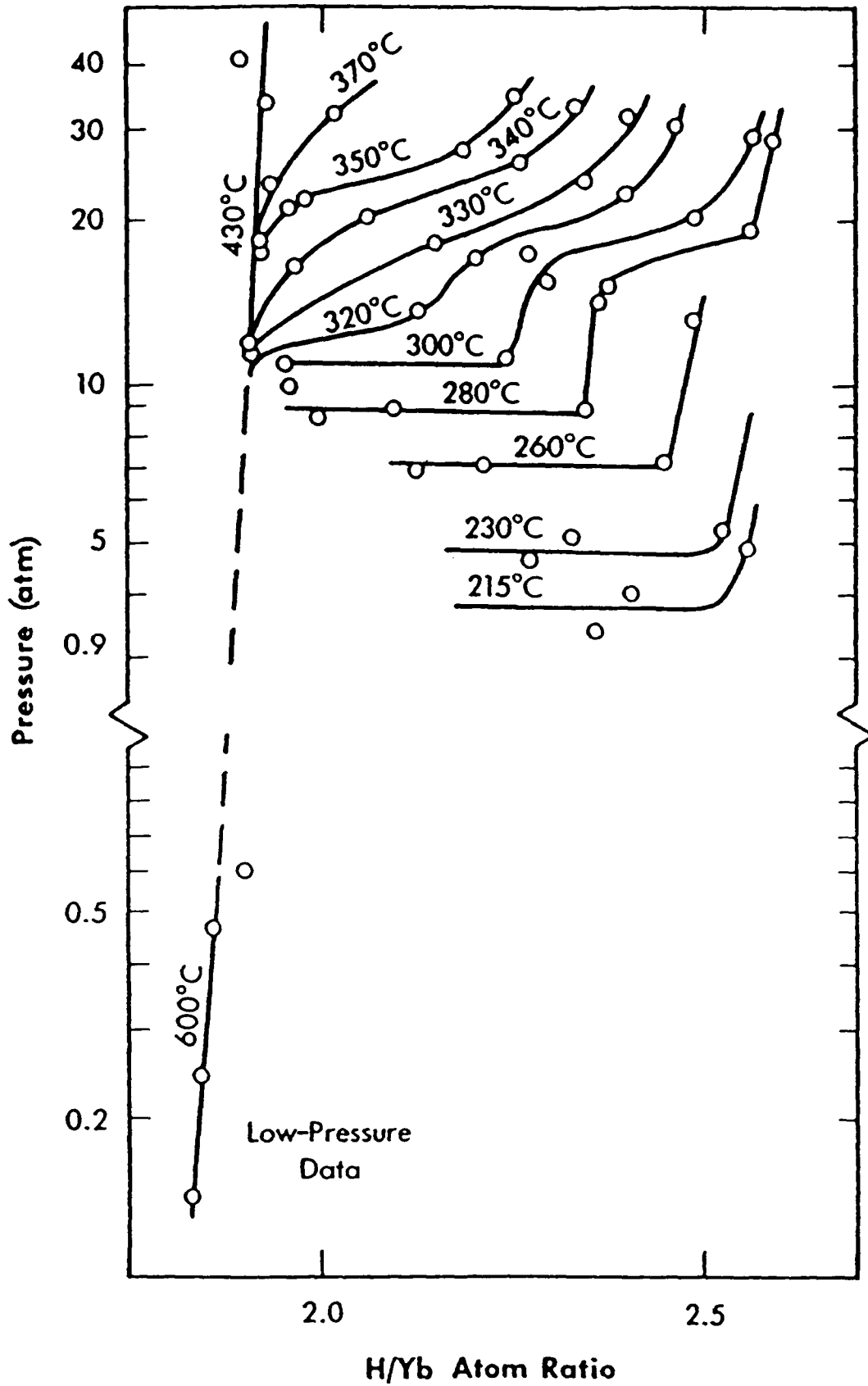


Fig. 28. Pressure-composition data for the ytterbium-hydrogen system.

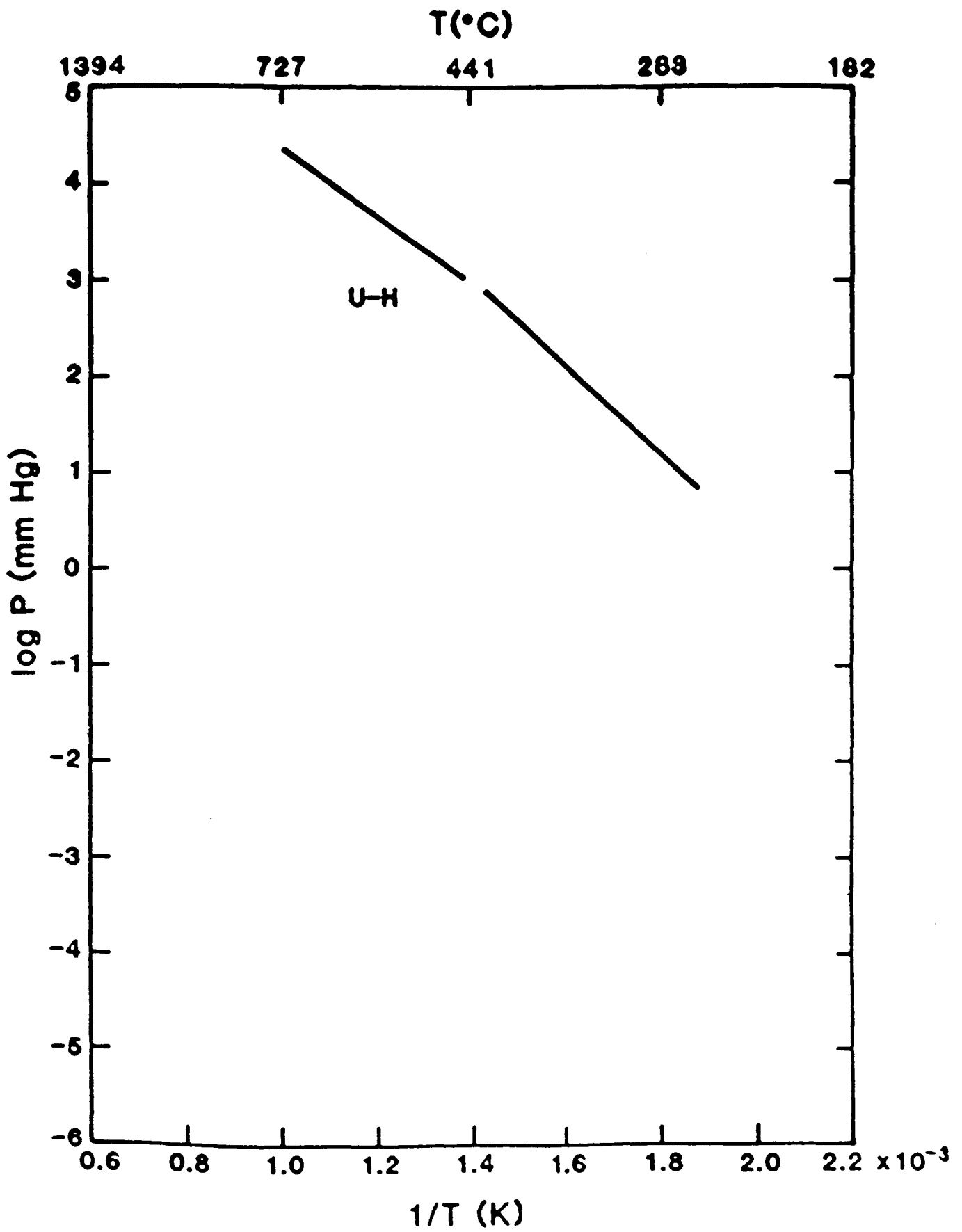


Fig. 29. Van't Hoff curve for the uranium-hydrogen system.

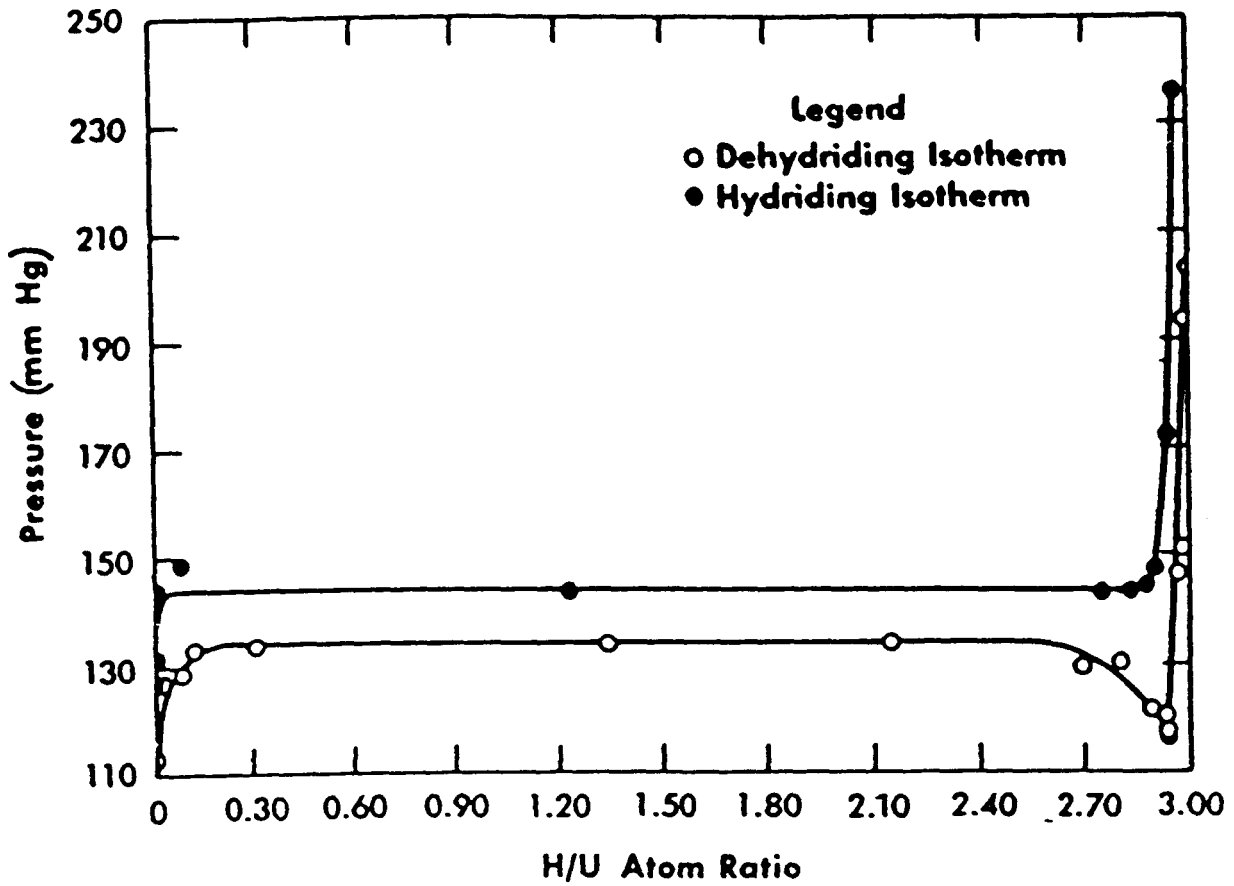


Fig. 30. Pressure-composition isotherm (357°C) for the uranium-hydrogen system.

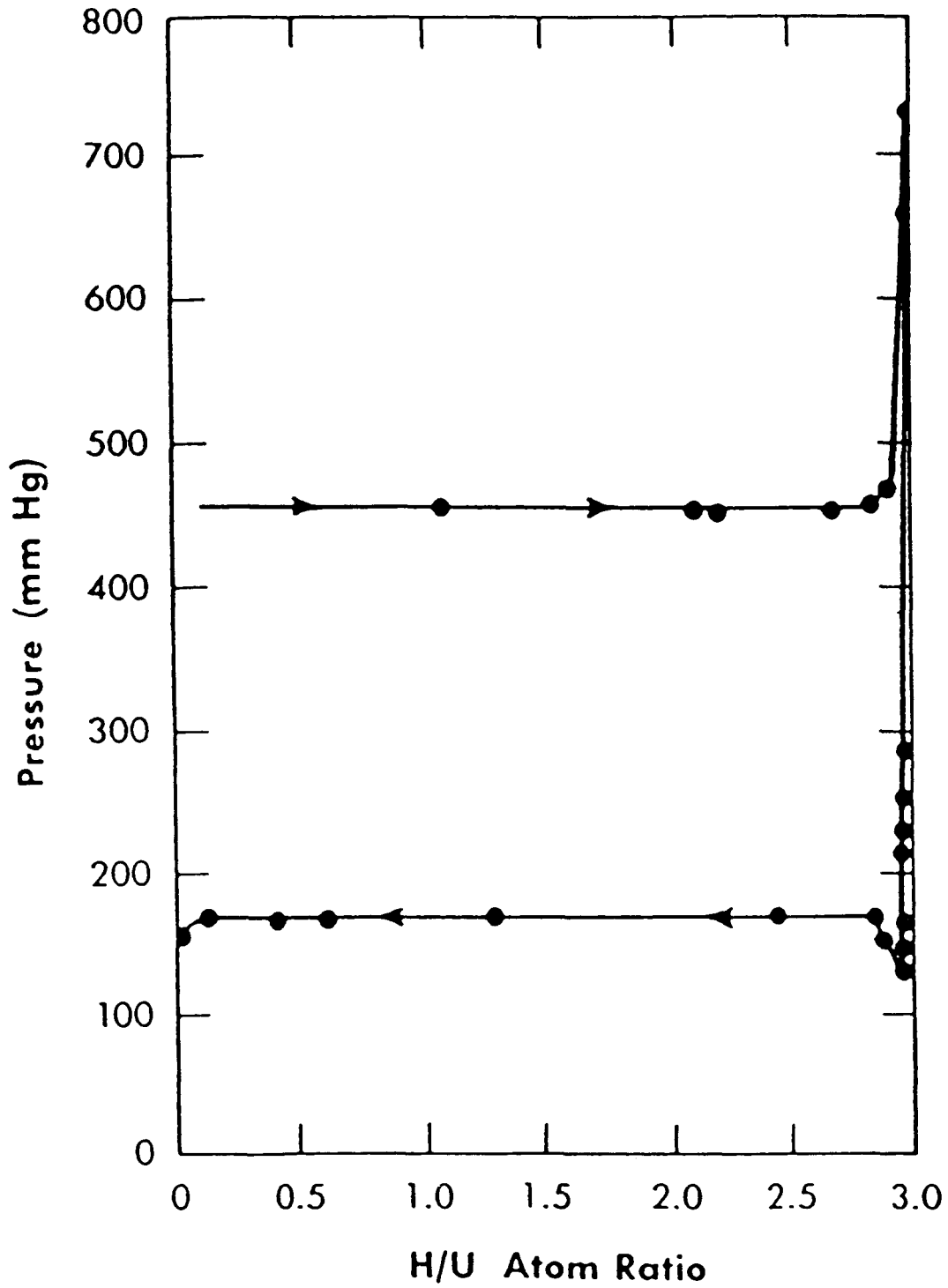


Fig. 31. Pressure-composition isotherm (369°C) for the uranium-hydrogen system.

Thorium hydride has not been investigated as thoroughly as uranium hydride. Its pressure plateaus slope upward with increasing hydrogen content, and these slopes are great enough that there is difficulty in determining the boundary of the one- and two-phase regions. Hydrogen solubility in thorium, however, is considerably greater than in uranium.

Negligible data are available for plutonium and neptunium.

E. Covalent Hydrides and Groups V Through VIII Transition Metals

Not many PCT data are available concerning these metal hydride systems, but of the known data, most of them concern the V-H, Nb-H, and Ta-H systems. Figure 32 shows the isobars of these three systems at 760 mm Hg and 1×10^{-5} mm Hg. These data are from the research of Edwards and Veleckis.³⁰ They used the following equations for these systems:

Vanadium

$$\ln(P^{1/2}) = 10.283 + 1.0598 \ln[r/(0.89-r)] + (-3489.2 - 3269r + 2563r^2 - 762.39r^3 + 4818.3r^4)/T, \quad (2)$$

Niobium

$$\ln(P^{1/2}) = 10.212 + 0.9841 \ln[r/(0.89-r)] + (-4244.7 - 4000.4r + 8872.7r^2 - 19338r^3 + 16230.3r^4)/T, \quad (3)$$

Tantalum

$$\ln(P^{1/2}) = 9.97 + 1.00311 \ln[r/(0.71-r)] + (-4051.4 - 3333.9r + 8350.7r^2 - 17057.2r^3 + 16951.4r^4)/T, \quad (4)$$

where

P = pressure (mm Hg),

T = temperature (K), and

r = H/M.

Table V summarizes the solubilities of the rest of the metals discussed. As can be seen, the solubility of hydrogen in these metals is low.

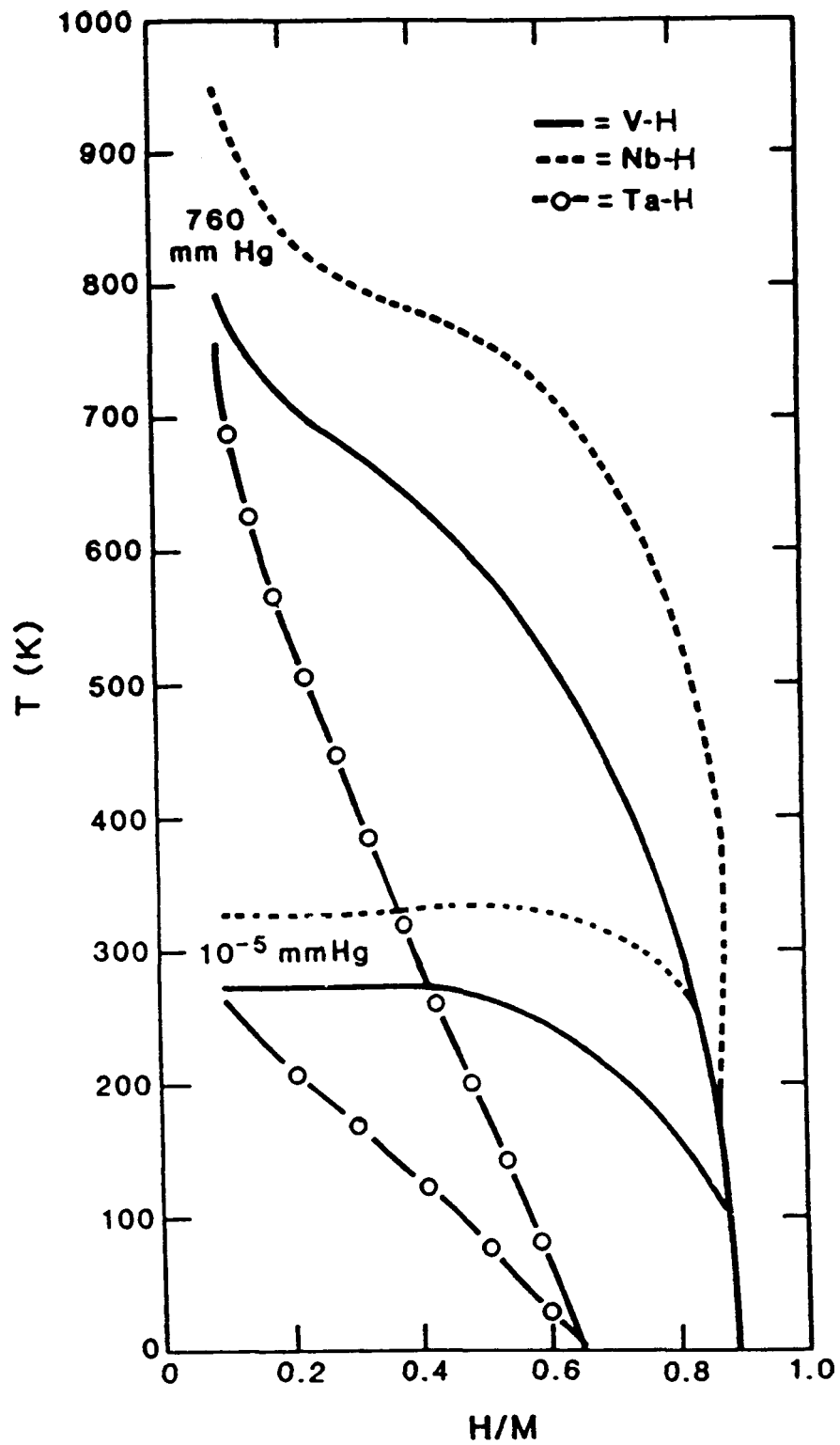


Fig. 32. Temperature-composition isobars for the vanadium-, niobium-, and tantalum-hydrogen systems.

TABLE V
COVALENT HYDRIDE SOLUBILITIES

<u>Element</u>	<u>T(°C)</u>	<u>P_{H2}(mm Hg)</u>	<u>H/M</u>
Lu	409	760	4×10^{-6}
Ag	400	800	5.5×10^{-6}
Al	400	760	2.4×10^{-8}
Sn	400	760	4.7×10^{-5}
Cr	400	760	1.3×10^{-5}
Co	600	753	4.7×10^{-5}
Pt	409	760	1.2×10^{-5}

III. ALLOYS

This section examines the PCT data for some metal alloys. We divide the metals into two categories: alloys with high equilibrium pressure at low temperatures and those with low equilibrium pressure. Feed-gas impurity effects are included in each section.

A. High-Pressure (>1 atm) Plateau Alloys

The two systems in this pressure range most often investigated are the La-Ni-H and Fe-Ti-H systems.

1. La-Ni-H Systems. The most common alloy of this group, LaNi₅, is easily activated and readily absorbs hydrogen at room temperature. Lanthanum, however, is costly and so other alloys have been made by substituting misch metals and magnesium for the lanthanum.

Uchida et al.³¹ investigated the systems La_{1-x}Re_xNi₅ (Re = La, Ce, Pr, Nd, or Sm). They found that adding these other metals to the alloy increases the pressure plateaus (Fig. 33) in proportion to the amount of rare earth present. The total amount of hydrogen absorbed, however, was constant. If investigators know the exact composition of the alloy, they can arrive at a good estimate of the equilibrium pressure. Conversely, they can engineer for this pressure by varying alloy composition.

Oesterreicher and Bittner³² investigated the system La_{1-x}Mg_xNi₂. These alloys hydride at room temperature up to H/M = 1.4. The Mg slows the kinetics of the reaction and thus decreases the rate of heat evolution for exothermic reactions. This action prevents decomposition of the intermetallic compound, which usually occurs because of high temperatures that result from the fast rate of reaction.

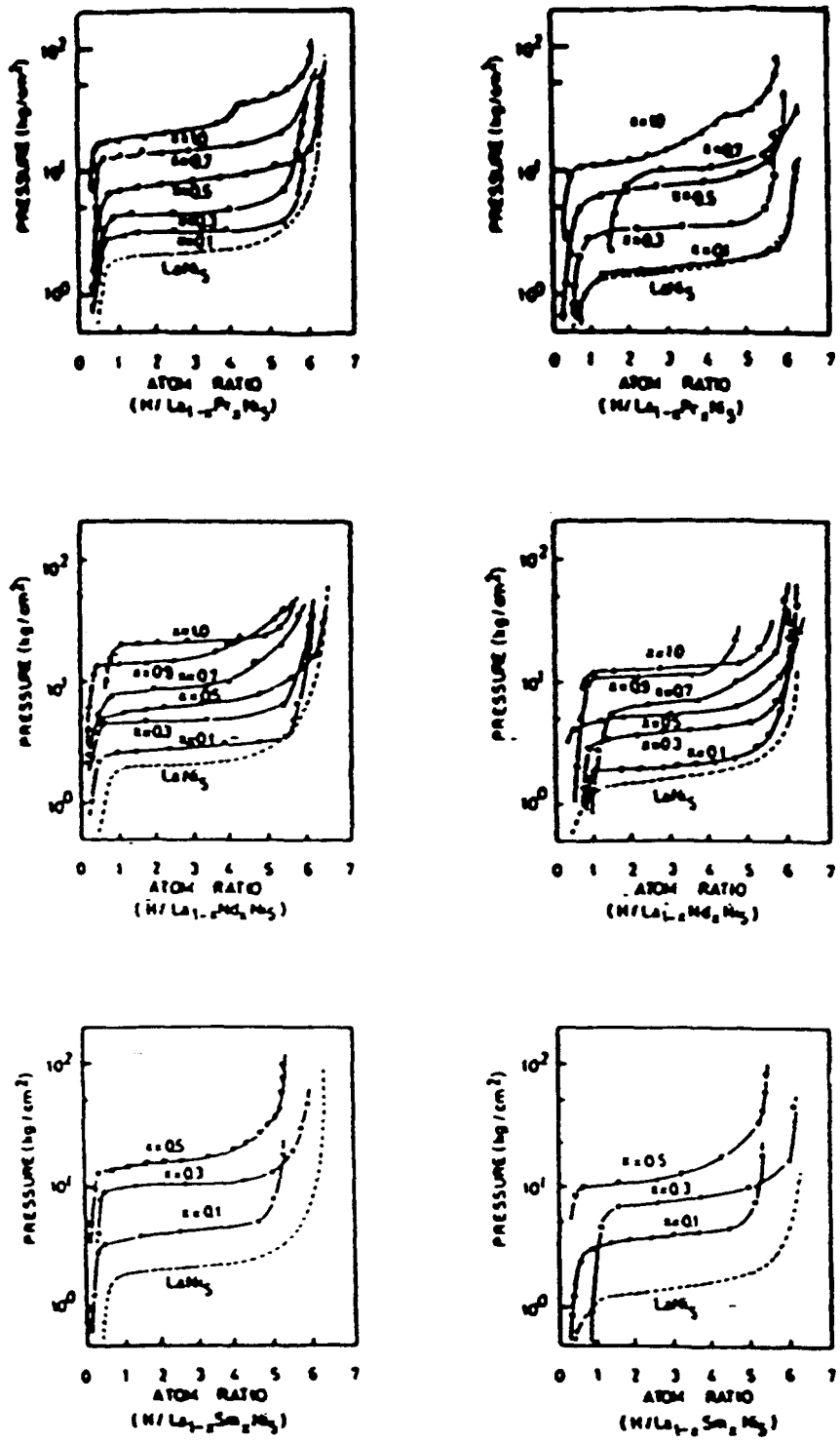


Fig. 33. Pressure-composition isotherms (293K) for $\text{La}_{1-x}\text{Re}_x\text{Ni}_5\text{-H}$ systems.

2. Fe-Ti-H System. The pressure-composition isotherm of annealed strain-free FeTi exhibits an absorption isotherm and two desorption isotherms, as shown in Fig. 34. Reilly et al.³³ found that the decrease in hydriding after many cycles was due to strain induced from cycling. The hydrogen capacity decreases from FeTi_{1.95} to a final steady-state value of FeTi_{1.5} independent of cycle number.

Amano et al.³⁴ report that splat quenching was used to produce FeTi_{1+x}O_y and FeTi_{1+x} flakes. It was found that these alloys had no pressure plateaus, though they did have hydriding characteristics similar to FeTi. The splat-quenched method appears to produce an alloy with a surface area larger than that of an annealed alloy.

Splat quenching could be applied to other alloys as well. It makes the alloys easier to pulverize and so decreases fabrication costs.

3. Selective Absorption by LaNi₅ and FeTi.³⁵ Impurities present in the feed gas often interact with the metal surface, impeding or preventing hydrogen absorption and dissociation. This interaction decreases the reaction rate because the poisoning causes a lowering of hydrogen capacity.

CH₄ and N₂ do not affect the hydrogen absorption rate significantly up to 20 vol% levels. CO₂ passivates LaNi₅ in concentrations up to 20 vol%; it deactivates FeTi, though reactivation with heat is possible. CO will deactivate both alloys in concentrations of less than 1 vol%. H₂S causes strong passivation effects in LaNi₅, but reactivation at 700 K is possible. H₂S poisons FeTi.

B. Low-Pressure (<1 atm) Plateau Alloys

This section examines several systems, including alloys of titanium, zirconium, magnesium, beryllium and uranium. Zirconium and titanium were the most common components of the alloys studied because of their good hydriding properties.

1. Titanium Alloys. The study of Mintz et al.³⁶ details the Ti₂MO_x (M = Fe, Co, Ni; 0 < x < 5) system. Pure Ti₂M compounds did not exhibit reproducible results. The decomposition curves occurred at 400°C ± 50°C. The investigators espouse several plausible reasons for this behavior: (1) TiM compounds exhibit extreme sensitivity to surface impurities, (2) surface layers of the disproportionation reactions act as resistances, (3) partial disproportionation occurs during heating with H₂, and (4) during cooling the titanium phase disproportionates into TiH₂ and TiM at the surface. Ti₂MO_x alloys, however, allow for reproducible results with an oxygen content of ≤5%. Figure 35 is a pressure-composition isotherm for the Zr-Co-H system for comparative purposes with the Ti-M-H systems. Comparison of alloys at 10 at.%

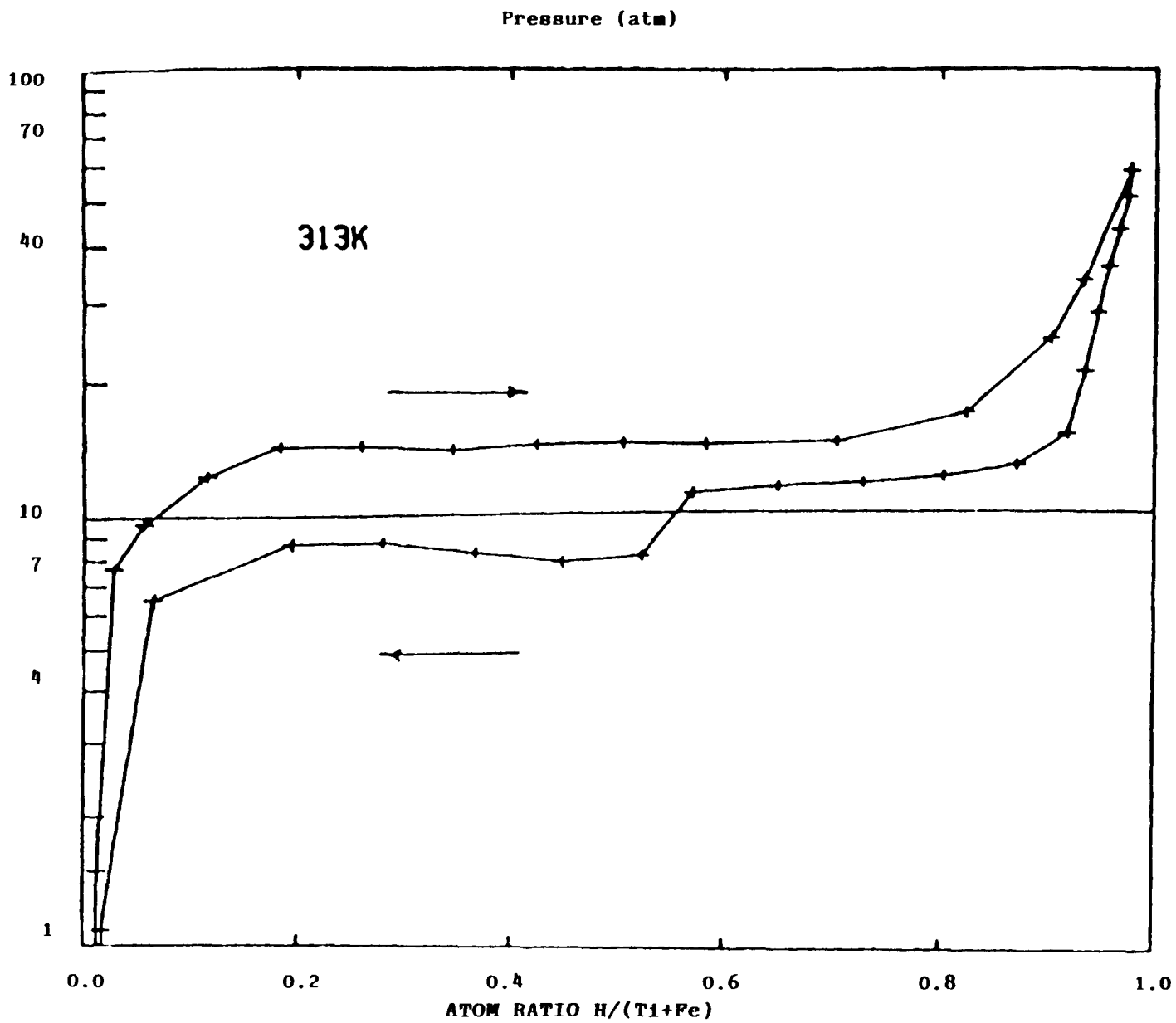


Fig. 34. Pressure-composition isotherm for the iron-titanium system.

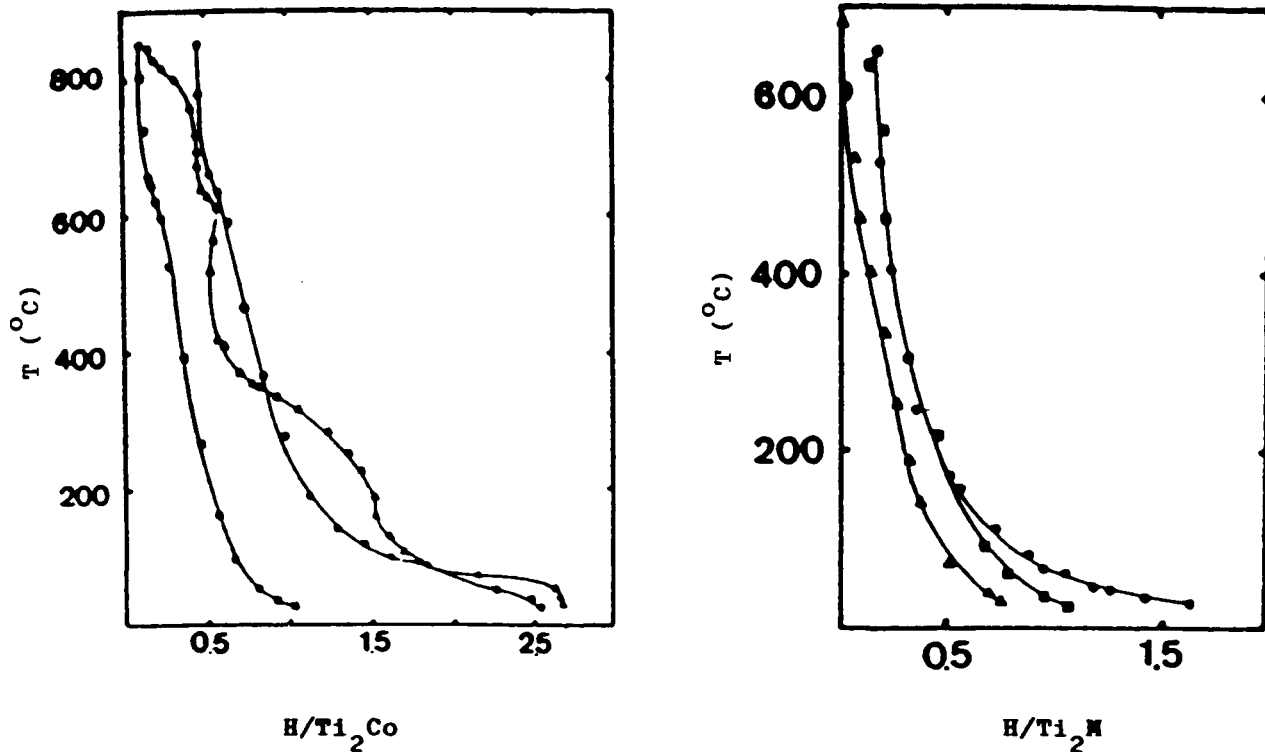


Fig 35. (a) Temperature-composition isobars (700 torr) for Ti_2CoO_x-H (Δ , $x = 0$; \bullet , $x = 0.18$; \blacksquare , $x = 0.33$).

(b) Temperature-composition isochores for $Ti_2MO_{.3}-H$ (\bullet , $M = Ni$; \blacksquare , $M = Co$; Δ , $M = Fe$).

oxygen shows that stability increases from iron to cobalt to nickel. Titanium alloyed with copper as $Ti_{.65}Cu_{.35}$ absorbed 35% more hydrogen when prepared as a glass rather than a crystal.

2. Zirconium Alloys. Irvine and Harris³⁷ investigated the Zr-Co and the Zr-Ni-Co systems. Figures 36 and 37 are PCT graphs for these systems. Hydrogenation of ZrCo occurs readily at 473 K and 200 mm Hg. At 298 K, pressure is approximately 6×10^{-3} mm Hg for the absorption isotherm. This low pressure points to the possible application of ZrCo in a tritium atmosphere.

Mendelsohn and Gruen³⁸ investigated alloys of the form AB_2 hoping that these alloys would provide low-pressure absorption as bulk getters. In particular, they studied $Zr(V_{1-x}Fe_x)_2$ alloys were studied ($x = 0.25, 0.3, \text{ and } 0.35$). Figure 38 shows isotherms for these alloys. The investigators found a linear correlation between the hydrogen equilibrium pressure and the amount of iron substituted: the less iron, the lower the pressure.

Saes Getters S.p.A. of Milan, Italy, has done in-depth work with zirconium getters. Two of its alloys, 84%Zr-16%Al (ST 101) and 70%Zr-24.6%V-5.4%Fe (ST 707), have good hydrogen sorption at very low pressures, as Figs. 39 and 40 show. Neither alloy showed any appreciable tendency to form fine particles after absorbing large doses of hydrogen, which is a desirable trait for tritium handling.

3. Magnesium Alloys. Magnesium alloys were investigated primarily because the lower weight of magnesium allows for a higher hydrogen weight capacity. Mintz et al.³⁹ added small amounts of Group III A metals to magnesium to try to improve hydriding characteristics over those of pure magnesium. Alloying increased the rate of activation (and the rate of hydriding after activation) because of the formation of oxide-free penetration sites on the surface of the reacting particles. The hydriding reaction rate is increased as the activation energy is cut in half for magnesium alloys containing about 0.4 at.% of a Group III A metal; this relationship is evidence of a valency effect. Pressure plateaus did not go into the very low pressure range; however, work must be done in that region to determine the alloys' tritium storage capability.

4. Beryllium Alloys. As with the magnesium alloys, beryllium alloys were studied⁴⁰ in hopes of finding a high-weight-efficiency hydriding alloy. Although all attempts to produce a rechargeable beryllium hydride by direct reaction of beryllium metal with hydrogen have failed, the alloys of Be_2Ti , Be_2Zr , and Be_2Hf do form definite hydride phases.

Be_2Ti is inactive at atmospheric pressure and room temperature. It is unstable and has a dissociation pressure between 1 and 150 atm at room temperature.

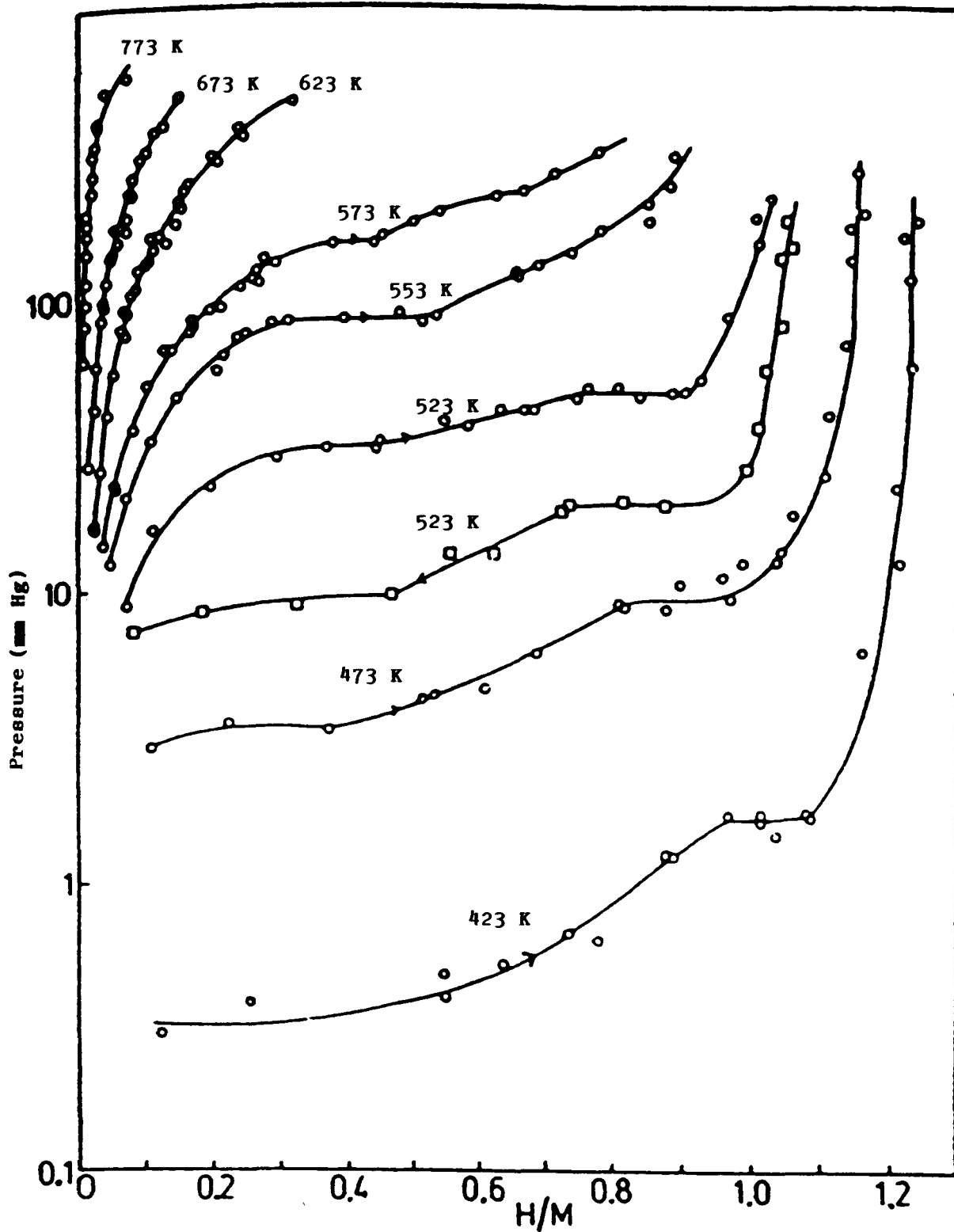


Fig. 36. Pressure-composition isotherms for the zirconium-cobalt-hydrogen system.

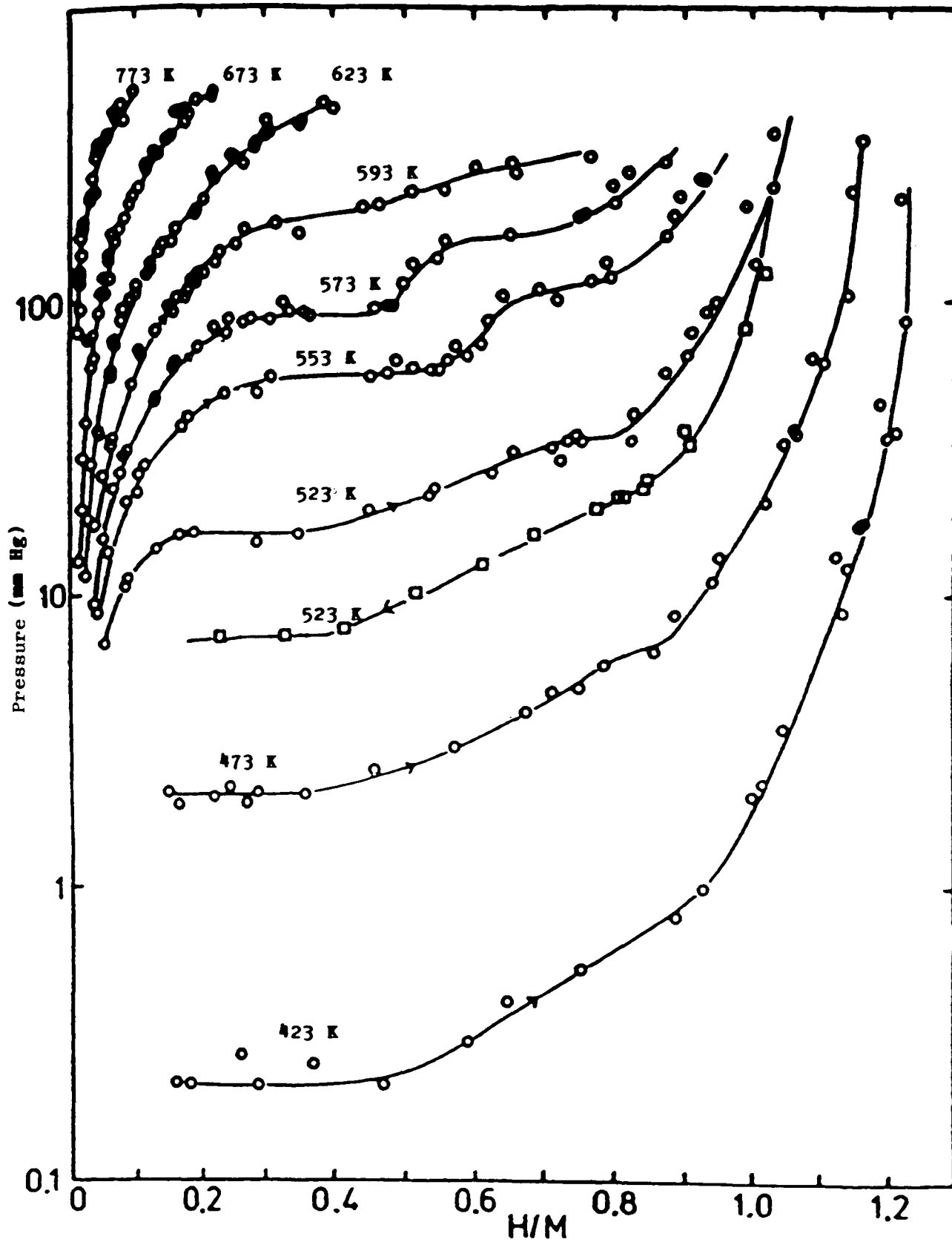


Fig. 37. Pressure-composition isotherms for the $\text{ZrCo}_{.84}\text{Ni}_{.16}\text{-H}$ system.

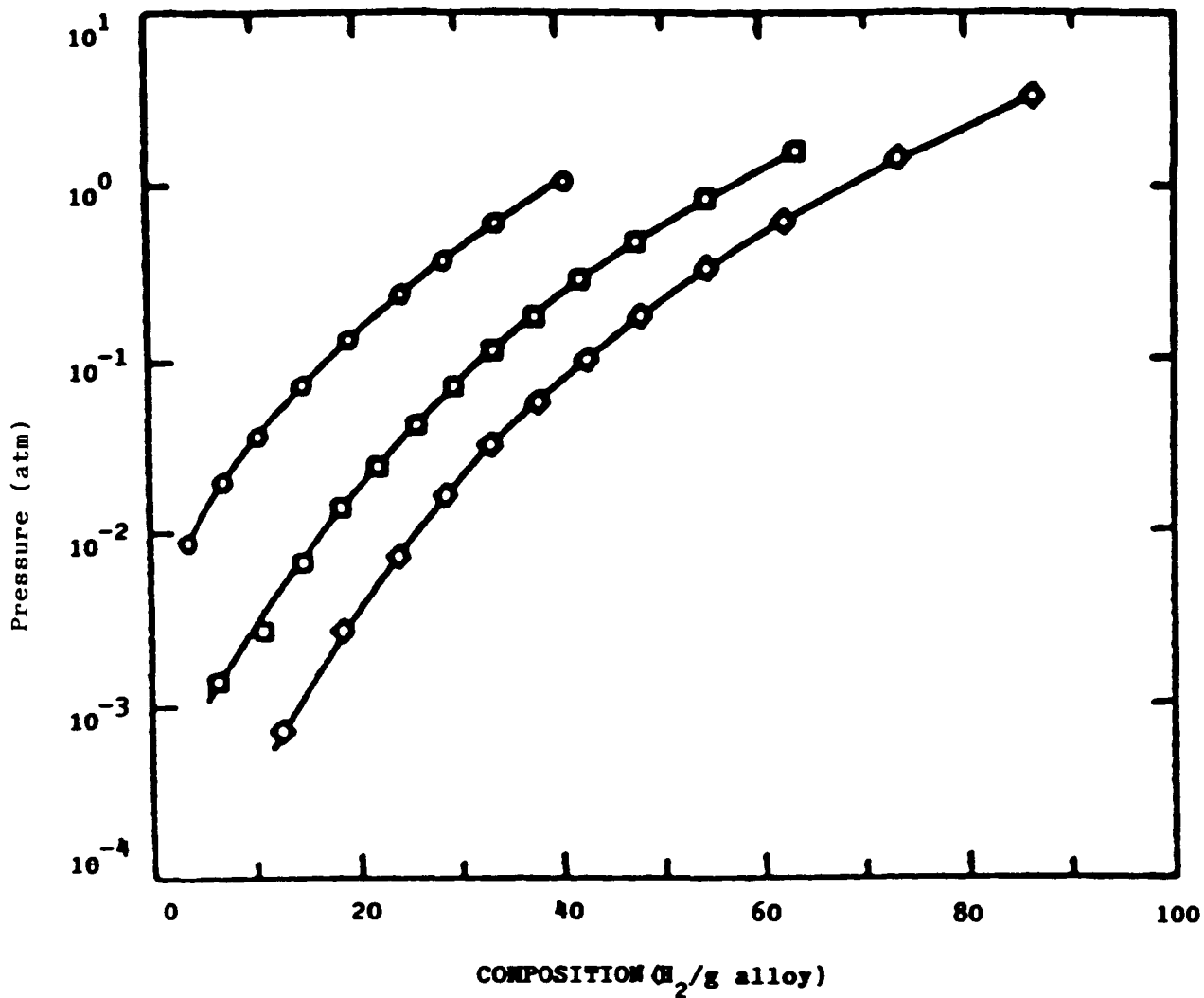


Fig. 38. Pressure-composition isotherms (400°C) for the $Zr(V_{1-x}Fe_x)_2$ systems (◊, $x = 0.25$; ■, $x = 0.30$; ○, $x = 0.35$).

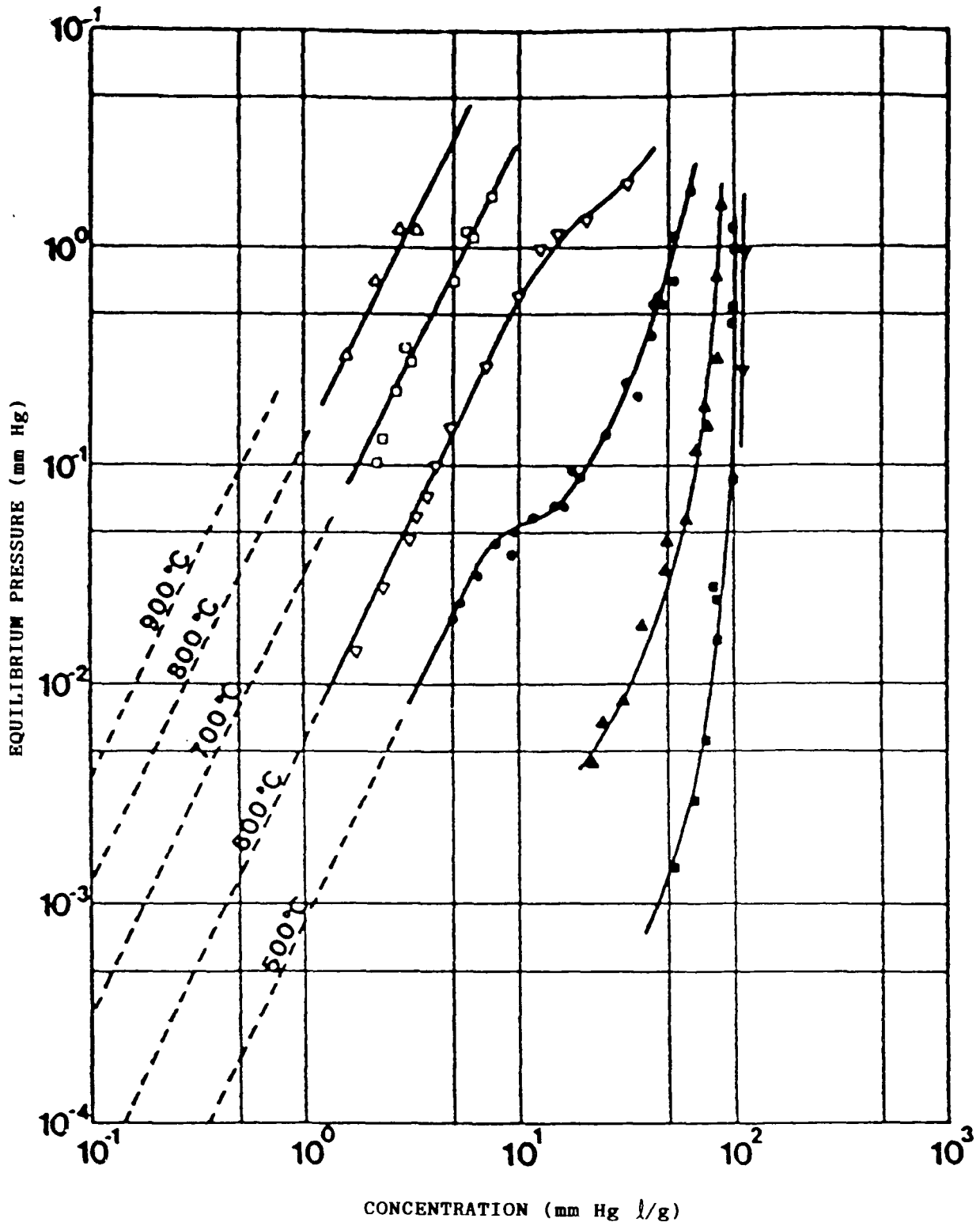


Fig. 39. Pressure-composition isotherms for the 84%Zr-16%Al system (ST 101) (∇ , 200°C; \square , 300°C, Δ , 400°C).

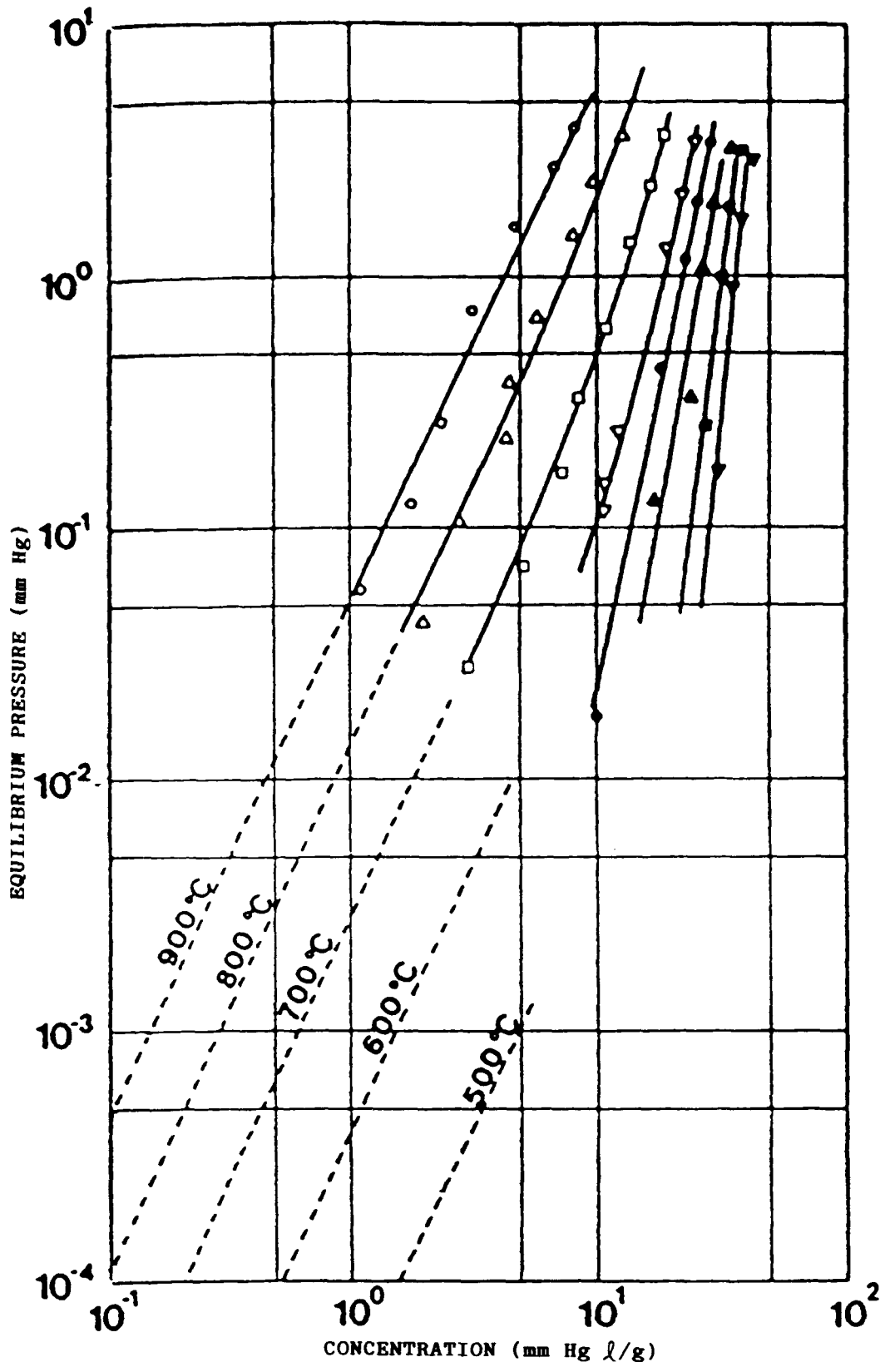


Fig. 40. Pressure-composition isotherms for the 70%Zr-24.6%V-5.4%Fe system (ST 707). The symbols are the same as in Fig. 39.

Be₂Zr reacts spontaneously at room temperature and atmospheric pressure to produce Be₂ZrH_{1.5}. The plateau pressure at room temperature was less than 0.8 mm Hg with a H/M ratio of up to 1.4.

Be₂Hf reacts similarly to Be₂Zr with hydrogen, except it has a lesser hydrogen content (Be₂HfH_{1.1}).

C. Impurity Removal and Effects

CO, a major poison of getter beds, seriously poisons La(Ni,Al)₅ and (Fe,Mn)Ti at 25°C.⁴¹ Degradation in hydriding rates of the alloys is exponential. At temperatures below 100°C the tolerance of the alloys to impurities is minimal, but reactivation is possible at higher temperatures. At higher temperatures (115°C-145°C), CO reacted with hydrogen and with LaNi₅ and (Fe,Mn)Ti surfaces to form CH₄. The CH₄ formation was essentially complete, so the direct poisoning effects of the CO were avoided. This temperature range increased the hydrogen transfer ability of the (Fe,Ni)Ti alloy. The Ti alloy was also less susceptible to irreversible bulk oxidation damage than La(Ni,Al)₅. It was more susceptible, however, to retardation of the rate of hydrogen absorption. Mg₂Ni was tested between 250°C and 350°C with high CO concentrations. The reaction of CO to CH₄ competes with the hydriding reaction for surface sites, causing rate retardation. Eventually the oxygen liberated in the methylation results in oxidation of the magnesium and alloy degradation.

Sandrock and Goodell⁴² tested LaNi₅, FeTi, and Fe.₈₅Mn.₁₅Ti for impurity surface poisoning at 10 torr. They concluded that (1) O₂ and H₂O produce very similar results; (2) FeTi and Fe.₈₅Mn.₁₅Ti show continuous poisoning in the presence of O₂ and H₂O, but LaNi₅ does not (After an initial partial loss of capacity, LaNi₅ almost completely recovers and then exhibits substantial immunity.); (3) CO is far more detrimental than either O₂ or H₂O to all three alloys; and (4) Fe.₈₅Mn.₁₅Ti reaches a steady-state level after which little additional damage is done. Surface poisoning appears to result from the formation of a surface structure that inhibits rapid catalytic hydrogen dissociation, perhaps covering active sites. Apparently, a wide variety of structures can result, depending on the alloy and the impurity gas.

REFERENCES

1. William M. Mueller, James P. Blackledge, and George G. Libowitz, Eds., Metal Hydrides (Academic Press, New York, 1968).
2. C. E. Messer, "A Survey Report on Lithium Hydride," USAEC report NYO-9470 (October 1960).
3. M. D. Banus, J. J. McSharry, and E. A. Sullivan, "The Sodium-Sodium Hydride-Hydrogen System at 500-600°," J. Am. Chem. Soc. 77, 2007-2010 (1955).
4. W. D. Treadwell and J. Sticher, "Uber den Wasserstoffdruck von Calcium-hydrid," Helv. Chim. Acta 36, 1820-1832 (1953).
5. J. F. Stampfer, Jr., C. E. Holley, Jr., and T. F. Suttle, "The Magnesium-Hydrogen System," J. Am. Chem. Soc. 82, 3504-3508 (1960).
6. F. K. Heumann and O. N. Salmon, "The Lithium Hydride, Deuteride, and Tritide Systems," Knolls Atomic Power Laboratory report KAPL-1667 (December 1956).
7. R. W. Curtis and P. Chiotti, "Thermodynamic Properties of Calcium Hydride," J. Phys. Chem. 67, 1061-1065 (1963).
8. A. Herold, "The Alkali Hydrides," Ann. Chim. (Paris) 6, 536-581 (1951).
9. W. C. Schumb, E. F. Sewell, and A. S. Eisenstein, "Observations on the Stability of the Barium-Hydrogen and Zirconium-Hydrogen Systems," J. Am. Chem. Soc. 69, 2029 (1947).
10. G. Hagg, "Rontgenuntersuchungen uber die Hydride von Titan, Zirkonium, Vanadin, and Tantal," Z. Phys. Chem. 11, 433 (1930).
11. S. L. H. Martin and A. L. G. Rees, "Interpretation of the Solubility of Hydrogen in Zirconium," Trans. Faraday Soc. 50, 343 (1954).
12. R. L. Beck, "Zirconium-Hydrogen Phase System," Trans. Am. Soc. Met. 55, 542 (1962); and "Thermophysical Properties of Zirconium Hydride," Trans. Am. Soc. Met. 55, 556 (1962).
13. G. G. Libowitz, "A Pressure-Composition-Temperature Study of the Zirconium-Hydrogen System at High Hydrogen Contents," J. Nucl. Mater. 5, 228 (1962).
14. L. D. LaGrange, L. J. Dykstra, J. M. Dixon, and U. Merten, "A Study of the Zr-H and Zr-H-U Systems Between 600°C and 800°C," J. Phys. Chem. 63(12), 2035 (1959).

15. E. A. Gulbranson and K. P. Andrew, "Solubility and Decomposition Pressure of Hydrogen in Alpha Zirconium," *Trans. Metall. Soc. AIME* 203, 136 (1955).
16. C. E. Ells and A. D. McQuillan, "A Study of the Hydrogen Pressure Relationships in the Zr-H System," *J. Inst. Met.* 85, 89 (1956).
17. R. L. Beck, "Research and Development of Metal Hydrides, Summary Report for October 1, 1958 to September 30, 1960," Denver Research Institute report LAR-10 (November 1960).
18. M. J. Trzeciak, D. F. Dilthey, and M. W. Mallett, "Study of Hydrides," Battelle Memorial Institute report BMI-1112 (July 1956).
19. R. K. Edwards and E. Veleckis, "Thermodynamic Properties in the System Hydrogen-Hafnium," *J. Phys. Chem.* 66, 1657 (1962).
20. T. R. P. Gibb, Jr., and H. W. Kruschwitz, Jr., "The Titanium-Hydrogen System and Titanium Hydride. I. Low Pressure Studies," *J. Am. Chem. Soc.* 72, 5365-5369 (1950).
21. C. E. Lundun and J. P. Blackledge, "Pressure-Temperature-Composition Relationships of the Yttrium-Hydrogen System," *J. Electrochem. Soc.* 109, 838-842 (1962).
22. L. N. Yannopoulos, R. K. Edwards, and P. G. Wahlbeck, "Thermodynamic Properties of the Yttrium-Hydrogen System," *J. Phys. Chem.* 69, 2510-2515 (1965).
23. W. L. Korst and J. C. Warf, "Rare Earth-Hydrogen Systems. I. Structural Thermodynamic Properties," *Inorg. Chem.* 5(10), 1719-1726 (1966).
24. R. N. R. Mulford and C. E. Holley, Jr., "Pressure-Temperature-Composition Studies of Some Rare Earth-Hydrogen Systems," *J. Phys. Chem.* 59, 1222 (1955).
25. G. E. Sturdy and R. N. R. Mulford, "The Gadolinium-Hydrogen System," *J. Am. Chem. Soc.* 73, 1083 (1956).
26. R. N. R. Mulford, "A Review of the Rare-Earth Hydrides," USAEC report AECU-3813. Los Alamos Scientific Laboratory.
27. J. C. Warf and K. I. Hardcastle, "Rare Earth-Hydrogen Systems. IV. The Higher Hydride of Ytterbium, A New Type of Hydride," *Inorg. Chem.* 5(10), 1736-1740 (1966).
28. F. H. Spedding et al., "Uranium Hydride. I. Preparation, Composition, Physical Properties," *Nucleonics* 4, 4 (1949).

29. E. Wicke and K. Otto, "The Uranium-Hydrogen System and the Kinetics of Hydride Formation," *Z. Phys. Chem. (Frankfurt am Main)* 31, 222 (1962).
30. R. K. Edwards and E. Veleckis, "The Thermodynamic Properties of the Systems: Nb-H, V-H, and Ta-H," 138th National Meeting of the American Chemical Society, New York, NY, September 1960; and E. Veleckis, Ph.D. thesis, Illinois Institute of Technology (January 1960).
31. H. Uchida, M. Tada, and Y. Huang, "The Influence of Cerium, Praseodymium, Neodymium and Samarium on Hydrogen Absorption in LaNi_5 Alloys," in Metal Hydrides 1982: Proceedings of the International Symposium on the Properties and Applications of Metal Hydrides, W. E. Wallace, T. Schober, and S. Suda, Eds. (Elsevier Sequoia, New York, 1983, Vol. I, pp. 81-88).
32. H. Oesterreicher and H. Bittner, "Hydride Formation in $\text{La}_{1-x}\text{Mg}_x\text{Ni}_2$," in Metal Hydrides 1980: Proceedings of the International Symposium on the Properties and Applications of Metal Hydrides, G. G. Libowitz and G. D. Sandrock, Eds. (Elsevier Sequoia, New York, 1980), Vol. I, pp. 334-339.
33. J. J. Reilly, J. R. Johnson, J. F. Lynch, and F. Reidinger, "Irreversible Effects in the FeTi-H System," in Metal Hydrides 1982: Proceedings of the International Symposium on the Properties and Applications of Metal Hydrides, W. E. Wallace, T. Schober, and S. Suda, Eds. (Elsevier Sequoia, New York, 1983), Vol. I, pp. 505-512.
34. J. Amano, R. Sasaki, R. Watanabe, and M. Shibata, "Hydrogen Storage Properties of FeTi_{1+x} and $\text{FeTi}_{1+x}\text{O}_y$ Flakes Produced by Splat Quenching," in Metal Hydrides 1982: Proceedings of the International Symposium on the Properties and Applications of Metal Hydrides, W. E. Wallace, T. Schober, and S. Suda, Eds. (Elsevier Sequoia, New York, 1983), Vol. II, pp. 513-518.
35. F. R. Brock and H. J. Bahs, "Investigation of Selective Absorption of Hydrogen by LaNi_5 and FeTi," in Metal Hydrides 1982: Proceedings of the International Symposium on the Properties and Applications of Metal Hydrides, W. E. Wallace, T. Schober, and S. Suda, Eds. (Elsevier Sequoia, New York, 1983), Vol. II, pp. 77-84.
36. M. H. Mintz, Z. Hadari, and M. P. Dariel, "Hydrogenation of Oxygen-Stabilized Ti_2MO_x (M = Fe, Co, Ni; $0_x.5$) Compounds," in Metal Hydrides 1980: Proceedings of the International Symposium on the Properties and Applications of Metal Hydrides, G. G. Libowitz and G. D. Sandrock, Eds., (Elsevier Sequoia, New York, 1980), Vol. II, pp. 287-294.

37. S. J. C. Irvine, and I. R. Harris, "An Investigation of the Systems $ZrCo-H_2$ and $ZrCo_{.84}Ni_{.16}-H_2$," in Metal Hydrides 1980: Proceedings of the International Symposium on the Properties and Applications of Metal Hydrides, G. G. Libowitz and G. D. Sandrock, Eds. (Elsevier Sequoia, New York, 1980), Vol. II, pp. 33-43.
38. M. H. Mendelsohn and D. M. Gruen, "Intermetallic Compounds as Bulk Getters," in Metal Hydrides 1980: Proceedings of the International Symposium on the Properties and Applications of Metal Hydrides, G. G. Libowitz and G. D. Sandrock, Eds. (Elsevier Sequoia, New York, 1980), Vol. II, pp. 449-453.
39. M. H. Mintz, Z. Gavra, and G. Kimmel, "The Reaction of Hydrogen with Magnesium Alloys and Magnesium Intermetallic Compounds," in Metal Hydrides 1980: Proceedings of the International Symposium on the Properties and Applications of Metal Hydrides, G. G. Libowitz and G. D. Sandrock, Eds. (Elsevier Sequoia, New York, 1980), Vol. I, pp. 263-270.
40. A. J. Maeland and G. G. Libowitz, "Hydrides of Beryllium-Based Intermetallic Compounds," in Metal Hydrides 1982: Proceedings of the International Symposium on the Properties and Applications of Metal Hydrides, W. E. Wallace, T. Schober, and S. Suda, Eds. (Elsevier Sequoia, New York, 1983), Vol. II, pp. 197-200.
41. F. G. Eisenberg and P. D. Goodell, "Cyclic Response of Reversible Hydriding Alloys in Hydrogen Containing Carbon Monoxide," in Metal Hydrides 1982: Proceedings of the International Symposium on the Properties and Applications of Metal Hydrides, W. E. Wallace, T. Schober, and S. Suda, Eds. (Elsevier Sequoia, New York, 1983), Vol. II, pp. 55-62.
42. G. D. Sandrock and P. D. Goodell, "Surface Poisoning of $LaNi_5$, $FeTi$ and $(Fe, Mn)Ti$ by O_2 , Co and H_2O ," in Metal Hydrides 1980: Proceedings of the International Symposium on the Properties and Applications of Metal Hydrides, G. G. Libowitz and G. D. Sandrock, Eds. (Elsevier Sequoia, New York, 1980), Vol. I, pp. 161-168.